# *Non-Linear Dynamics of Mooring Lines*

by

GENEVIEVE TCHEOU

B.S. in Mechanical Engineering
*University Joseph Fourier, Grenoble, France. (1993)*

M.S. in Mechanical Engineering
*Ecole Nationale Supérieure de Techniques Avancées, Paris, France. (1995)*

Submitted to the Department of Ocean Engineering
in partial fulfillment of the requirements for the degree of

**Master of Science in Ocean Engineering**

at the

MASSACHUSETTS INSTITUTE OF TECHNOLOGY

June 1997



Author .....
Department of Ocean Engineering
May 9, 1997

Certified by .....
Paul D. Sclavounos
Professor of Naval Architecture
Thesis Supervisor

Accepted by .....
Kim Vandiver
Chairman, Departmental Committee on Graduate Students

# *Non-Linear Dynamics of Mooring Lines*

by

GENEVIEVE TCHEOU

Submitted to the Department of Ocean Engineering
on May 9, 1997, in partial fulfillment of the
requirements for the degree of
**Master of Science in Ocean Engineering**

## Abstract

Offshore platforms are often maintained in position by multipoint mooring systems, which resist environmental loads from all directions. Therefore, the statics and dynamics of the supporting cables of compliant structures are of primary importance in studying the behavior of the overall system.

The objective of this thesis is to investigate an approximate method based on multiple scale theory in order to model as efficiently as possible the dynamics of mooring lines.

The motion of a mooring line is decomposed into a mean static component, a wave frequency component with a small amplitude and quickly varying time dependency and a slow-drift component with a large amplitude and slowly varying time dependency. Assuming that the response of this stable physical system to a harmonic excitation is periodic and considering the different scales as separate excitations, the motion of the cable can be expressed as a Fourier series for each component.

Starting from the general expression of the equation of motion of a mooring line in a global coordinate system and from specified boundary conditions, equations for the Fourier coefficients $\vec{C}_{kn}$ of the response to each forcing are derived. The prediction of the motion of the cable for several excitation frequencies, cable materials, and forcing directions is then performed numerically for the static and the dynamic cases.

Thesis Supervisor: Paul D. Sclavounos
Title: Professor of Naval Architecture

# Contents

# List of Tables

# List of Figures

# CHAPTER 1

# INTRODUCTION

## 1.1 Background

The interaction between floating offshore structures and their mooring systems is essential in designing the overall system. Therefore, a good understanding of both the dynamics of the cables and of offshore platforms is a major concern. This thesis develops an analytical model for the behavior of a mooring line based on multiple scale theory. Some theoretical background on offshore platforms and mooring lines is presented in the first two following sections.

### 1.1.1 Offshore platforms

Oil producing offshore platforms are designed to operate at a stationary position over or near the oil well(s). Floating platforms are typically large volume structures which support their weight through floatation. They are compliant in that they maintain their position via a system of mooring lines or tethers.

The design of compliant offshore platforms intended to operate in large water depths over long time periods requires the understanding and modeling of the linear and non-linear environmental wave loads and the ability to simulate the platform and mooring system responses over several-hour intervals for use in design. A compliant offshore structure moored or tethered to the ocean floor typically undergoes large am-

plitude slow-drift oscillations, as well as small amplitude wave frequency oscillations, about its mean position. This slow-drift response is driven by the low-frequency non-linear wave effects. Two important tasks faced by the designer of an offshore platform are the determination of the wave induced loads and the resulting structure responses. They are needed for the structural design of the platform and the mooring system.

Since the development at MIT over the past 15 years of the computer program WAMIT (Wave Analysis MIT), the solution of the linearized interaction of ambient waves with general purpose offshore structures is widely regarded as complete.

The hydrodynamic forces responsible for the large amplitude responses of compliant offshore structures are of non-linear nature and are dominated by second-order surface wave effects. Two types of forces must be determined for the eventual prediction of the large amplitude slow-drift responses of the structure, the slow-drift excitation and wave drift damping.

Over the past 5 years, a computer program named SWIM has been developed for the prediction of the linear wave effects, slow-drift excitation, and wave drift damping of multi-leg offshore structures. With the set of rational, approximate, analytical techniques implemented in SWIM, particular emphasis was placed in achieving a balance between accuracy, robustness, and efficiency for the method to be of utility in offshore structure design where slow-drift response records of several hours long are necessary. SWIM permits the easy and efficient evaluation of all the linear and second-order hydrodynamic quantities governing the slow-drift oscillation of offshore platforms.

A set of non-linear differential equations governing the slow-drift responses of compliant structures, in directional sea states, in all six rigid-body motions, and in the time domain, have been developed and coded into the computer program MOTION. An essential property of MOTION is that all relevant hydrodynamic effects, namely the slow-drift excitation and wave drift damping coefficient, are all evaluated in the frequency domain a priori and independently of the instantaneous orientation of the structure in the course of the slow-drift simulation. This allows MOTION to accept hydrodynamic input from SWIM and then proceed to carry out slow-drift motion

simulations several hours long efficiently in realistic sea states. For example, a 10-hour long simulation of the slow drift motion of a realistic structure in a directional sea state by MOTION requires about 1 hour of CPU time on a Pentium PC.

The viscous excitation and damping as well as the mooring line restoring coefficients can also modeled in MOTION. This program was designed to be a flexible and efficient linear and slow-drift motion simulation code which may be coupled with available hydrodynamic and mooring line computer programs.

However, the mooring line damping model implemented in SWIM relies on certain restricting assumptions, such as the quasistatic dynamic deformation of the line or the linearized transverse displacements at small wave frequencies, see [4]. In order to fully simulate the motion of compliant offshore structures using the above software, a complete mooring line model is essential. This work is concerned with the development of a non-linear, fully dynamic model for mooring lines, which may be coupled with SWIM or MOTION to get the response of the overall system including the offshore platform along with its mooring system. The main goal of the method, described in this thesis, is to establish a set of accurate and efficient techniques, similar to those used in SWIM, in order to take into account the non-linear effects of mooring lines dynamics.

### 1.1.2 Mooring Systems

The offshore industry makes a wide use of cables and long flexible cylinders (risers and flexible pipelines) that have cable-like dynamic behavior. Mooring systems are one of the marine applications of cables. Floating offshore platforms are often maintained in position by a multipoint mooring system with anywhere from 4 to 16 mooring lines, arranged in a radial fashion about the platform.

As the oil supplies get depleted, the necessity to produce oil from greater depths will become more pressing and, with it, the need for larger platforms and therefore for longer and stronger cables, capable of resisting environmental loads from all directions, operating in adverse environments will increase. The statics and dynamics of the supporting cables of compliant structures are of primary importance in study-

ing the behavior of these systems. In fact, reliable and well designed models for the dynamics of the lines are essential in order to make offshore platforms safe and economical to build and operate.

Normally, the effects of mooring lines are ignored in computing linear (wave frequency) motions of offshore platforms. But in computing the slow-drift motions, the proper modeling of the mooring lines is important for two reasons. First, the mooring lines provide the only restoring forces in the horizontal plane. Second, the mooring lines may contribute significantly to the damping of the slow-drift motions. Each mooring line has a significant non-linear force - displacement characteristic.

There are many studies in the literature concerning the dynamic behavior of platform and their moorings. Although these studies have attempted to interpret the impact of the mooring on the overall platform performance, it is difficult to generalize these results in terms of the issues which confront the mooring designer. The conduct of model tests of moored platforms is particularly difficult. In those cases where the tank is large enough to include the whole moor, the model scale is such that the mooring lines have a very small diameter. Matching the physical properties of the mooring lines is tedious but possible. Assuring that the hydrodynamic forces are correctly modeled is more difficult.

In many cases, the mooring system is replaced with mechanical springs chosen to match the static non-linear characteristics of the mooring line. When this approach is followed, the dynamic behavior of the mooring lines is clearly not modeled. The difficulties encountered in the study of marine cables stem not only from the involved structural equations describing the cable but also from the interaction between the cable and the surrounding fluid. This non-linear interaction complicates the problem to a great extent. Actually, the complexity of the dynamics of a single mooring line resides in the non-linearity of the governing partial differential equations with variable coefficients forces. Employing numerical techniques at a very early stage results in significant consequences for the cost and flexibility of the design procedure, while simplistic models lead to unreliable predictions.

### 1.1.3 Multiple Scale Model

The analytical model developed in this report is based on an mathematical approach. The objective is to investigate an approximate method based on multiple scale theory, along the lines of Emmerhoff and Sclavounos [2], where a multiple scale model is used for the evaluation of the slow-drift response of a compliant floating structure. The method can then be able to be coupled with computer programs such as SWIM and MOTION described above, in order to model as efficiently as possible the dynamics of mooring lines.

The formulation of the equation of motion for a single mooring line is based on the theory of a flexible cable presented by Nordgren [5] and later by Garrett [3]. In this analysis, the instantaneous configuration of a cable is expressed as a vector distance $\vec{r}(s,t)$, from the origin of an inertial coordinate system as a function of s, the arc length along the mooring line, and time t. Using the expression of the equation of motion in a global coordinate system is one characteristic of this approach in order to simplify the formulation of the equations. Other models including the fully non-linear dynamics of mooring lines in a local coordinate system have been developed, see [8]. The theory assumes the cable to be elastic but can have an arbitrary geometry. Further expansions, by Paulling and Webster [6], included various loadings encountered in marine applications as well as the extensibility condition of a mooring line. These forces consist of the forces on the cable due to hydrodynamic effects resulting from the cable motion and the fluid motion, the effect of pressure gradients in the fluid, and the weight of the cable.

The motion of a mooring line is decomposed into a mean static component, a wave frequency component characterized by its small amplitude and fast varying time dependency and a slow-drift component which has a large amplitude and varies slowly in time.

Assuming that the response of a stable physical system to a harmonic excitation is periodic, and considering the different scales as separate excitations, the motion of the cable can be expressed into a Fourier series for each forcing frequency. The purpose is

to determine the Fourier coefficients of the response to each forcing in order to predict the motion of the cable for all the different excitation frequencies needed to be taken into account. Starting from the equation of motion given by Webster [9], equations will be derived for the Fourier coefficients $\vec{C}_k$ and their solution will be carried out numerically for given cable boundary conditions and physical characteristics, for the static and dynamic cases.

This study focuses on a single mooring line. The fairlead is assumed to be at the free surface and is oscillated sinusoidally at various amplitudes and frequencies to determine the response of the mooring line.

## 1.2 Overview

This thesis has been divided into six chapters.

Chapter two covers the analytical formulation of the problem, beginning with the general formulation, in a global coordinate system, of the equation of motion for a single mooring line, followed by the expression of the extensibility of a mooring line. Then, the multiple scale approach, based on a Fourier analysis, is described and finally, approximated sets of equations, neglecting the contribution of the bending stiffness, are derived for the static and the dynamic motions.

Chapter three specifies the cable configuration, starting with the graphical and mathematical description of the boundary conditions for the static and dynamic cases. For this particular closed boundary value problem, analytical solutions for an inelastic and an elastic cable are then derived for the static case, by solving the catenary equations.

Chapter four discusses the numerical aspects encountered during the transition process from the mathematical formulation to the numerical implementation. The discretization of the equation of motion, involving finite difference schemes, is first detailed. Then, the Newton-Raphson method used to solve these equations is described. And finally, initial guesses of the cable configuration, essential for the iterative process of the previous method, are presented for both the static and dynamic cases.

Chapter five illustrates numerical results for various tests cases. First, material properties of the cable and the fluid are given for a basis case. For the static case, simulations are presented for steel materials with Young's modulus of $10^{10}N/m^2$. Convergence results have been achieved by varying the total number of elements on the cable and by comparing with the analytical solutions obtained in chapter three. For the dynamic case, similar kinds of simulations have been conducted for the slow-drift and wave frequency motions, where the fairlead oscillates harmonically in the horizontal direction. The results are compared to the static motion in order to identify the linear and second-order contributiuon in the displacement.

Finally, the last chapter outlines the main conclusions and the future work topics.

# CHAPTER 2

# MATHEMATICAL FORMULATION

## 2.1 Nomenclature

The symbols and expressions used in the derivation of the equation of motion in the following sections are given in table (2.1).

## 2.2 General Equation of Motion

This section outlines the derivation of the equation of motion which will be used in the multiple scale analysis and expresses the condition of extensibility of the cable.

### 2.2.1 Formulation

This formulation uses symbols and expressions defined in table (2.1). Consider a cable shown in figure (2-1), where the vector $\vec{r}(s,t)$ represents the position of a point on the centerline of the cable, as a function of arc length s and time t.

For an inextensible cable, the motion is governed by:

$$\begin{cases} m\ddot{\vec{r}} + (B\vec{r}'')'' - (T\vec{r}')' &= \vec{q} \\ \\ \vec{r}' \cdot \vec{r}' &= 1 \end{cases} \tag{2.1}$$

| | | |
|---|---|---|
| $\vec{r}(s,t)$ | = | position vector of the cable |
| $m(s) = \rho_s A_s$ | : | cable mass per unit length |
| $A_s$ | = | cable structural cross-sectional area |
| $\rho_s$ | = | mass density of the cable |
| $B(s) = EI_s$ | : | cable bending rigidity |
| $E$ | = | Young's modulus of elasticity |
| $I_s$ | = | moment of inertia in bending |
| $T(s,t)$ | = | instantaneous local tension in the cable |
| $\vec{q}(s,t)$ | = | distributed force on the cable per unit length |
| $\vec{g} = g\,\vec{e}_z$ | : | acceleration due to gravity |
| $A_f$ | = | cross-sectional area for estimating the added mass forces |
| $C_d$ | = | cross-flow drag coefficient based on $D_f$ |
| $C_m$ | = | added-mass coefficient based on $A_f$ |
| $D_f$ | = | effective diameter for estimating hydrodynamic drag |
| $\rho_f$ | = | mass density of sea water |
| $\vec{v_f}(s,t)$ | = | fluid velocity at s |
| $\vec{v}(s,t)$ | = | mooring line velocity at s |
| $\widetilde{M} = \rho_s A_s + \rho_f A_f C_m \mathcal{N}$ | : | effective mass matrix |
| $\mathcal{N} = \mathcal{I} - (\vec{r}')^T \vec{r}'$ | : | mathematical operator |
| $\tilde{\lambda} = T + P_f A_f$ | : | effective tension |
| $T_e = T + P_e A_s$ | = | tension including hydrostatic pressure |
| $P_e$ | = | hydrostatic pressure in the neighborhood of a cable element |
| $P_f$ | = | total pressure, including both hydrostatic and acceleration of the fluid induced pressures |

Table 2.1: Nomenclature

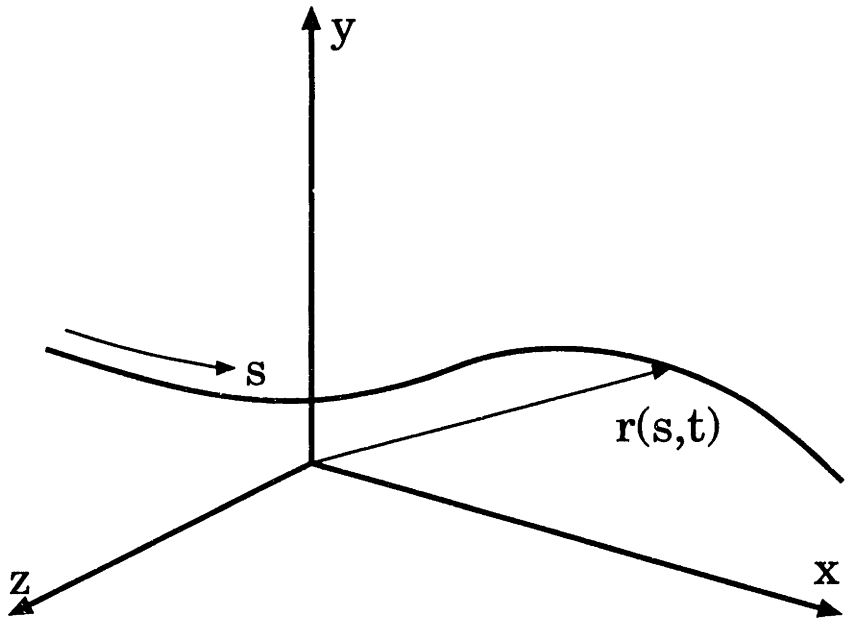


Figure 2-1: Definition of $\vec{r}(s,t)$

Eq. (2.1), describing the conservation of linear momentum, assumes that no fluid exists inside the mooring line.

The mooring line is exposed to many loadings. The major ones are the effect of gravity on the mass of the cable and the hydrodynamic forces due to the cable motion and the wave motion. The hydrodynamic forces are composed of an added mass force and a damping force (estimated by the Morison equation) and a Froude-Krylov force.

The effect of gravity on the mass of the cable leads to :

$$\vec{q}_s = \rho_s A_s \vec{g} \tag{2.2}$$

The acceleration component of the hydrodynamic forces is given by :

$$\vec{q}_f^{accel} = \rho_f A_f C_m \mathcal{N} \left( \vec{v}_f - \vec{v} \right) \tag{2.3}$$

where the normal component of any vector $\vec{x}$ is expressed by $x_n = \vec{x} - (\vec{x} \cdot \vec{r'})\vec{r'} = \mathcal{N}\vec{x}$, with $\mathcal{N} = \mathcal{I} - (\vec{r'})^T \vec{r'}$ and $\mathcal{I}$ the identity matrix.

The hydrodynamic damping term is :

$$\vec{q}_f^{damp} = \frac{1}{2}\rho_f D_f C_d \left|\vec{v}_n^{rel}\right| \vec{v}_n^{rel} \tag{2.4}$$

where $\vec{v}_n^{rel} = \mathcal{N}(\vec{v}_f - \vec{v})$ is the relative velocity.

The Froude-Krylov force includes the buoyancy effect, the effect due to the acceleration of the fluid, including an additional term arising from the pressure on the cable surface. This total force yields :

$$\vec{q}_f^{F-K} = \rho_f A_f \left(\vec{g} + \dot{\vec{v}}_f\right) + \left(P_f A_f \vec{r}'\right)' \tag{2.5}$$

Substituting all the forces eq.(2.2), eq.(2.3), eq.(2.4) and eq.(2.5) in the right hand side of the equation of motion of the cable eq.(2.1), the general equation of motion in the global coordinate system becomes :

$$\widetilde{M}\ddot{\vec{r}} + \left(B\vec{r}''\right)'' - \left(\tilde{\lambda}\vec{r}'\right)' = \begin{cases} \rho_f A_f \left(1 + C_m \mathcal{N}\right) \dot{\vec{v}}_f \\ \\ +\frac{\rho_f}{2} C_d D_f \vec{v}_n^{rel} \left|\vec{v}_n^{rel}\right| \\ \\ +g\left(\rho_f A_f - \rho_s A_s\right) \vec{e}_z \end{cases} \tag{2.6}$$

where the first term on the right hand side of the equation is the fluid inertia, the second is the drag and the last is related to the net weight of the cable in water per unit length.

### 2.2.2 The stretch condition

Mooring lines are likely to be composed of materials which have relatively small, but non-negligible, elastic elongations, like various steels and synthetics. Therefore, it is necessary to express an approximate stretch condition of the cable.

Let $s_1$ be the stretched arclength and s the unstretched arclength along the cable centerline, the tangent vector $\vec{t}(s,t)$ to the cable is given by expression (2.7).

$$\begin{aligned} \vec{t} &= \frac{\partial \vec{r}}{\partial s_1} \\ &= \frac{\partial \vec{r}}{\partial s} \times \frac{ds}{ds_1} \end{aligned} \tag{2.7}$$

The strain $\epsilon(s,t)$ at the point s of the cable is defined as :

$$\begin{aligned} \epsilon &= \frac{ds_1 - ds}{ds} \\ &= \frac{ds_1}{ds} - 1 \end{aligned} \tag{2.8}$$

The cables display a linear stress-strain relation with a constant Young's modulus E. Hooke's law relates the strain with the stress at the point s of the cable :

$$\begin{cases} \sigma = E\epsilon \\ \sigma = \dfrac{T_e}{A_s} \end{cases} \tag{2.9}$$

$$\Longrightarrow \quad \epsilon = \frac{T_e}{EA_s} \tag{2.10}$$

From eq.(2.7), eq.(2.8), eq.(2.9) and eq.(2.10), the following expression for $\vec{r}'(s,t)$, the rate of change of the cable position vector with respect to the unstretched arclength along the cable, or in other words, the rate of stretch of the cable, is deduced:

$$\begin{aligned} \vec{r}' &= \frac{\partial \vec{r}}{\partial s} \\ &= \vec{t}\,\frac{ds_1}{ds} \\ &= (1+\epsilon)\vec{t} \\ &= (1+\frac{T_e}{EA_s})\vec{t} \end{aligned} \tag{2.11}$$

For a small extension of the cable, it follows from eq.(2.8) and eq.(2.10) that $\frac{T_e}{EA_s} \ll 1$.

From the expression of $\vec{r}'(s,t)$, eq.(2.11), and under the assumption $\frac{T_e}{EA_s} \ll 1$, the following scalar equation describes the stretch condition :

$$\begin{aligned} \vec{r}' \cdot \vec{r}' &= \left(1 + \frac{T_e}{EA_s}\right)^2 \vec{t} \cdot \vec{t} \\ &\approx 1 + 2\frac{T_e}{EA_s} \end{aligned} \tag{2.12}$$

Since $\vec{t}$ is a unit vector, $\vec{t} \cdot \vec{t} = 1$.

Note that if $\epsilon \approx 0$, or the cable is nearly inextensible, the previous consition becomes :

$$\vec{r}' \cdot \vec{r}' = 1 \tag{2.13}$$

From the stretch condition eq.(2.12), the tension is determined by :

$$T_e = \frac{EA_s}{2}\left(\vec{r}' \cdot \vec{r}' - 1\right) \tag{2.14}$$

It is therefore possible to solve for the position vector of the cable using the equation of motion and to then determine the instantaneous value of the tension at each point. Note that if the cable is inextensible, $\vec{r}' \cdot \vec{r}' = 1$ and $E \gg 1$, therefore, the preceding expression (2.14) is not used to determine the tension anymore. For the static case, the tension is obtained through the resolution of the catenary equations, given in chapter three. Since these equations can be solved analytically, the tension is defined exactely, via the boundary conditions, and there is no need to use an approximate expression to compute it. For the dynamic case, the problem needs to be formulated differently in order to calculate the tension.

## 2.3 Multiple Scale Decomposition

The motion of a mooring line is decomposed into a mean static component, a wave frequency component which has a small amplitude and varies quickly in time and a slow-drift component with a large amplitude and a slowly varying time dependency as follows :

$$\vec{r}(s,t) = \vec{r}_o(s) + \vec{r}_1(s,t) + \vec{r}_2(s,t)$$

where the time dependency of $\vec{r}_1$ and $\vec{r}_2$ is respectively in $\omega_1$, wave frequency, and $\omega_2$, slow-drift frequency.

### 2.3.1 Fourier Decomposition

Assuming that the response of a stable physical system to a harmonic excitation is periodic, and considering the different scales as separate excitations, the motion of the cable can be expressed as a Fourier series for each component, in the following form :

$$\begin{cases} \vec{r}_o(s) &= \vec{C}_o(s) \\ \\ \vec{r}_k(s,t) &= \sum_{n=-\infty}^{+\infty} \vec{C}_{kn}(s)\ e^{in\omega_k t} \quad , \text{k} = 1,2. \end{cases} \tag{2.15}$$

The purpose is to determine the Fourier coefficients of the response to each forcing in order to predict the motion of the cable for all the different excitation frequencies which need to be taken into account.

Equations for the Fourier coefficients $\vec{C}_{kn}$ are derived by substituting $\vec{r}_k(s,t)$ for its expressions (2.15) in each member of the equation of motion eq.(2.6). In the following sections, the static problem and then the dynamic case will be developed in detail. For both the static and the dynamic cases, the bending rigidity term plays a

secondary role in the mooring line motion and can therefore be ignored.

### 2.3.2 Static Motion

The static case where the motion of the cable is time independent, only depends on space, the curvilinear coordinate $s$. The solution of this problem is necessary not only in order to validate the approximate model with analytical solutions but also will be used to initialize the dynamic motion.

The position vector is given according to the Fourier decomposition eq.(2.15) as follows: $\vec{r}(s) = \vec{C}_o(s)$.

#### Restoring of the mooring line

From the expression of $T_e$ (2.14) and its definition, the instantaneous tension T is given by :

$$T = \frac{EA_s}{2}(\vec{r}' \cdot \vec{r}' - 1) - P_e A_s \tag{2.16}$$

The effective tension $\tilde{\lambda} = T + P_f A_f$ can be expressed in terms of $\vec{r}(s)$ since the total pressure $P_f$ is reduced to the hydrostatic pressure $P_e$, in the static case. Therefore,

$$\tilde{\lambda} = \frac{EA_s}{2}(\vec{r}' \cdot \vec{r}' - 1) \tag{2.17}$$

The resulting restoring term for the static case, knowing $\vec{r}(s) = \vec{C}_o(s)$, is finally :

$$\begin{aligned} \left(\tilde{\lambda}\vec{r}'\right)' &= \left(\frac{EA_s}{2}\left(\vec{C}_o' \cdot \vec{C}_o' - 1\right)\vec{C}_o'\right)' \\ &= \frac{EA_s}{2}\left(\left(\vec{C}_o' \cdot \vec{C}_o'\right)\vec{C}_o'\right)' - \frac{EA_s}{2}\vec{C}_o'' \end{aligned} \tag{2.18}$$

#### Equation of motion

The response of the mooring line is only composed of the restoring effects since the bending rigidity term has been neglected, and since there is no acceleration of the

cable, the equation of motion leads to :

$$-(\tilde{\lambda}\vec{r}')' = \vec{g}(\rho_f A_f - \rho_s A_s) \tag{2.19}$$

Substituting the restoring term eq.(2.18), found in the preceding section, into the left hand side of eq.(2.19) results in the following :

$$-\frac{E A_s}{2}\left(\left(\vec{C}_o' \cdot \vec{C}_o'\right)\vec{C}_o'\right)' + \frac{E A_s}{2}\vec{C}_o'' - g(\rho_f A_f - \rho_s A_s)\vec{e}_z = \vec{0} \tag{2.20}$$

The gravity $\vec{g}$ is disctributed over all the elements in the same way, so that the equations in the x and z directions are as follows :

- *In the x direction :*

$$\frac{E A_s}{2}\left(\left(\vec{C}_o' \cdot \vec{C}_o'\right)\vec{C}_o'\right)_x' - \frac{E A_s}{2}C_{ox}'' = 0 \tag{2.21}$$

- *In the z direction :*

$$-\frac{E A_s}{2}\left(\left(\vec{C}_o' \cdot \vec{C}_o'\right)\vec{C}_o'\right)_z' + \frac{E A_s}{2}C_{oz}'' + g(\rho_s A_s - \rho_f A_f) = 0 \tag{2.22}$$

### 2.3.3 Dynamic Motion

The two dynamic motions of concern are the wave frequency and the slow-drift motions. Therefore, the position vector is both a function of time $t$ and of the curvilinear coordinate $s$ and is given by the Fourier decomposition eq.(2.15).

For each component of the multiple scale decomposition, characterized by its frequency $\omega$, the instantaneous configuration of the cable $\vec{r}(s,t)$ is expressed by:

$$\vec{r}(s,t) = \sum_{k=-n}^{n} \vec{C}_k(s)\, e^{ik\omega t}, \quad n \to +\infty \tag{2.23}$$

### Inertia of the mooring line

The acceleration term of the mooring line is given by :

$$\begin{aligned} \widetilde{M}\ddot{\vec{r}} &= (\rho_s A_s + \rho_f A_f C_m \mathcal{N})\,\ddot{\vec{r}} \\ &= (\rho_s A_s + \rho_f A_f C_m)\,\ddot{\vec{r}} - \rho_f A_f C_m \left(\vec{r'} \cdot \ddot{\vec{r}}\right) \vec{r'}. \end{aligned} \tag{2.24}$$

The expression $\left[\left(\vec{r'} \cdot \ddot{\vec{r}}\right) \vec{r'}\right]$ is evaluated in appendix A of this thesis.

Subsituting eq.(2.23) into eq.(2.24) leads to the inertia term of the cable for a dynamic motion of frequency $\omega$ :

$$\begin{aligned} \widetilde{M}\ddot{\vec{r}} &= -(\rho_s A_s + \rho_f A_f C_m)\,\omega^2 \sum_{s=-n}^{n} s^2 \vec{C}_s e^{is\omega t} \\ &+\rho_f A_f C_m \omega^2 \sum_{s=-3n}^{3n} \left[ \sum_{t=-2n}^{2n} \left( \sum_{q=-n}^{n} q^2 \vec{C}_q \cdot \vec{C}'_{t-q} \right) \vec{C}'_{s-t} \right] e^{is\omega t} \end{aligned} \tag{2.25}$$

where the conditions of existence for the Fourier coefficients are,

$$\begin{cases} \vec{C}'_{t-q} = \vec{0} \quad for\ t-q > n\ and\ t-q < -n \\ \vec{C}'_{s-t} = \vec{0} \quad for\ s-t > n\ and\ s-t < -n \end{cases} \tag{2.26}$$

### Restoring of the mooring line

Recall that the tension T can be expressed by :

$$T = \frac{EA_s}{2}(\vec{r'} \cdot \vec{r'} - 1) - P_e A_s \tag{2.27}$$

And the effective tension $\tilde{\lambda}$ by :

$$\tilde{\lambda} = \frac{EA_s}{2}(\vec{r'} \cdot \vec{r'} - 1) \tag{2.28}$$

The derivation of $\left(\vec{r'} \cdot \vec{r'}\right)$ is obtained in appendix A, at the end of this thesis.

Substituting eq.(2.23) into eq.(2.28) yields the restoring term for a motion of frequency $\omega$ :

$$\begin{aligned}\left(\tilde{\lambda}\vec{r'}\right)' &= \left(P_f A_f - \frac{EA_s}{2} - P_e A_s\right) \sum_{s=-n}^{n} \vec{C}''_s e^{is\omega t} \\ &+ \frac{EA_s}{2} \sum_{s=-3n}^{3n} \left[ \sum_{t=-2n}^{+2n} \left( \sum_{q=-n}^{n} \vec{C}'_q \cdot \vec{C}'_{t-q} \right) \vec{C}'_{s-t} \right]' e^{is\omega t}\end{aligned} \tag{2.29}$$

where

$$\begin{cases} \vec{C}'_{t-q} = \vec{0} \quad for\ t-q > m\ and\ t-q < -m \\ \vec{C}'_{s-t} = \vec{0} \quad for\ s-t > m\ and\ s-t < -m \end{cases} \tag{2.30}$$

### Response of the mooring line

The overall response of the mooring line is composed of the inertia and the restoring effects since the bending rigidity term has been neglected.

Therefore, substituting the inertia term eq.(2.25) and the restoring term eq.(2.29) into the left hand side of the general equation of motion eq.(2.6), results in the expression (2.31), which represents the response of the mooring line.

$$
\begin{aligned}
\widetilde{M}\ddot{\vec{r}} - (\tilde{\lambda}\vec{r}')' &= -(\rho_s A_s + \rho_f A_f C_m)\,\omega^2 \sum_{s=-n}^{n} s^2 \vec{C}_s e^{is\omega t} \\
&+\rho_f A_f C_m \omega^2 \sum_{s=-3n}^{3n} \left[ \sum_{t=-2n}^{2n} \left( \sum_{q=-n}^{n} q^2 \vec{C}_q \cdot \vec{C}'_{t-q} \right) \vec{C}'_{s-t} \right] e^{is\omega t} \\
&-\left( P_f A_f - \frac{EA_s}{2} - P_e A_s \right) \sum_{s=-n}^{n} \vec{C}''_s e^{is\omega t} \\
&-\frac{EA_s}{2} \sum_{s=-3n}^{3n} \left[ \sum_{t=-2n}^{2n} \left( \sum_{q=-n}^{n} \vec{C}'_q \cdot \vec{C}'_{t-q} \right) \vec{C}'_{s-t} \right]' e^{is\omega t}
\end{aligned}
\tag{2.31}
$$

where,

$$
\begin{cases}
\vec{C}'_{t-q} = \vec{0} \quad for\ t-q > n\ and\ t-q < -n \\
\vec{C}'_{s-t} = \vec{0} \quad for\ s-t > n\ and\ s-t < -n
\end{cases}
\tag{2.32}
$$

### Exciting Forces

Assuming that the fluid is stationary so that no forcing from the fluid velocity exists, the only dynamic force on the cable due to its motion in fluid is the drag force.

The expression for the drag force, from eq.(2.6), is :

$$
F_D = \frac{\rho_f}{2} C_d D_f \vec{v}_n^{rel} \left| \vec{v}_n^{rel} \right| \tag{2.33}
$$

For a stationary fluid, the relative velocity can be written as :

$$
\begin{cases}
\vec{v}_n^{rel} &= -\mathcal{N}\dot{\vec{r}} \\
&= -\left( \dot{\vec{r}} - (\dot{\vec{r}} \cdot \vec{r}')\vec{r}' \right)
\end{cases}
\tag{2.34}
$$

The relative velocity $\vec{v}_n^{rel}$ as well as the general expression of the drag force are derived in appendix A.

Substituting eq.(2.34) into eq.(2.33), and considering the expression of the relative velocity eq.(A.33), the drag force is obtained :

$$\begin{aligned} F_D &= -i\omega^2 \frac{\rho_f}{2} C_d D_f \\ &\left( \sum_{s=-n}^{n} \vec{C}_s \, s \; e^{is\omega t} - \sum_{s=-3n}^{3n} \left[ \sum_{t=-2n}^{2n} \left( \sum_{q=-n}^{n} q \, \vec{C}_q \cdot \vec{C}'_{t-q} \right) \vec{C}'_{s-t} \right] e^{is\omega t} \right) \\ &\cdot \left| \sum_{s=-n}^{n} \vec{C}_s \, s \; e^{is\omega t} - \sum_{s=-3n}^{3n} \left[ \sum_{t=-2n}^{2n} \left( \sum_{q=-n}^{n} q \, \vec{C}_q \cdot \vec{C}'_{t-q} \right) \vec{C}'_{s-t} \right] e^{is\omega t} \right| \end{aligned} \tag{2.35}$$

with the following conditions of existence for the Fourier coefficients :

$$\begin{cases} \vec{C}'_{t-q} = \vec{0} \quad for \; t-q > n \; and \; t-q < -n \\ \\ \vec{C}'_{s-t} = \vec{0} \quad for \; s-t > n \; and \; s-t < -n \end{cases} \tag{2.36}$$

### Equation of motion

The approximated equation of motion of a mooring line is obtained by neglecting the bending rigidity of the cable. The response of the cable is given by the expression (2.31) while three kinds of forcing for the right hand side have been treated.

- *With drag :*

  For a stationary fluid, the total pressure $P_f$ is reduced to the hydrostatic pressure $P_e$, therefore the response of the cable, eq.(2.31), can be simplified. Assuming that the drag force is taken into account, the resulting equation of motion is given by eq.(2.37).

$$\widetilde{M}\vec{\ddot{r}} - (\tilde{\lambda}\vec{r}')' = \frac{\rho_f}{2} C_d D_f \vec{v}_n^{rel} \left| \vec{v}_n^{rel} \right| \tag{2.37}$$

The developed form is :

$$\left\{ \begin{array}{l} -\left(\rho_s A_s + \rho_f A_f C_m\right) \omega^2 \sum_{s=-n}^{n} s^2 \vec{C}_s e^{is\omega t} \\ \\ +\rho_f A_f C_m \omega^2 \sum_{s=-3n}^{3n} \left[ \sum_{t=-2n}^{2n} \left( \sum_{q=-n}^{n} q^2 \vec{C}_q \cdot \vec{C}'_{t-q} \right) \vec{C}'_{s-t} \right] e^{is\omega t} \\ \\ +\frac{EA_s}{2} \sum_{s=-n}^{n} \vec{C}''_s e^{is\omega t} \\ \\ -\frac{EA_s}{2} \sum_{s=-3n}^{3n} \left[ \sum_{t=-2n}^{2n} \left( \sum_{q=-n}^{n} \vec{C}'_q \cdot \vec{C}'_{t-q} \right) \vec{C}'_{s-t} \right]' e^{is\omega t} \end{array} \right.$$

$$= \left\{ \begin{array}{l} -i\omega^2 \frac{\rho_f}{2} C_d D_f \\ \\ \left( \sum_{s=-n}^{n} \vec{C}_s \, s \, e^{is\omega t} - \sum_{s=-3n}^{3n} \left[ \sum_{t=-2n}^{2n} \left( \sum_{q=-n}^{n} q \vec{C}_q \cdot \vec{C}'_{t-q} \right) \vec{C}'_{s-t} \right] e^{is\omega t} \right) \\ \\ \cdot \left| \sum_{s=-n}^{n} \vec{C}_s \, s \, e^{is\omega t} - \sum_{s=-3n}^{3n} \left[ \sum_{t=-2n}^{2n} \left( \sum_{q=-n}^{n} q \vec{C}_q \cdot \vec{C}'_{t-q} \right) \vec{C}'_{s-t} \right] e^{is\omega t} \right| \end{array} \right.$$

where,

$$\left\{ \begin{array}{lcl} \vec{C}'_{t-q} & = & \vec{0} \quad for \; t-q > n \; and \; t-q < -n \\ \\ \vec{C}'_{s-t} & = & \vec{0} \quad for \; s-t > n \; and \; s-t < -n \end{array} \right.$$

The identification of the exponential terms would lead to a system of non-linear time independent equations. Each system of equations would yield a solution for the Fourier coefficients $\vec{C}_k$ for each frequency. However, the expression of this system is very complex and can hardly be simplified in order to proceed to any identification.

- *Without drag :*

  One alternative is to ignore the drag along with the fluid inertia force. Although, the fluid exciting forces, such as the inertia and the drag, are not modeled, the full non-linear behavior of the structural cable is accounted for in this case. The mooring line then follows a dynamic motion given by the equation :

$$\widetilde{M}\ddot{\vec{r}} - (\tilde{\lambda}\vec{r}')' = \vec{0} \tag{2.38}$$

The developed form gives :

$$\vec{0} = \left\{ \begin{array}{l} -(\rho_s A_s + \rho_f A_f C_m)\,\omega^2 \sum_{s=-n}^{n} s^2\,\vec{C}_s e^{is\omega t} \\ \\ +\rho_f A_f C_m\,\omega^2 \sum_{s=-3n}^{3n} \left[ \sum_{t=-2n}^{2n} \left( \sum_{q=-n}^{n} q^2\,\vec{C}_q \cdot \vec{C}'_{t-q} \right) \vec{C}'_{s-t} \right] e^{is\omega t} \\ \\ +\dfrac{EA_s}{2} \sum_{s=-n}^{n} \vec{C}''_s e^{is\omega t} \\ \\ -\dfrac{EA_s}{2} \sum_{s=-3n}^{3n} \left[ \sum_{t=-2n}^{2n} \left( \sum_{q=-n}^{n} \vec{C}'_q \cdot \vec{C}'_{t-q} \right) \vec{C}'_{s-t} \right]' e^{is\omega t} \end{array} \right. \tag{2.39}$$

For each frequency, i.e. for a given s where $-3n < s < +3n$, identifying the exponential terms yields :

$$\vec{0} = \begin{cases} -\left(\rho_s A_s + \rho_f A_f C_m\right) \omega^2 l^2 \vec{C}_l \\ +\rho_f A_f C_m \omega^2 \left[\sum_{t=-2n}^{2n} \left(\sum_{q=-n}^{n} q^2 \vec{C}_q \cdot \vec{C}'_{t-q}\right) \vec{C}'_{l-t}\right] \\ +\frac{EA_s}{2} \vec{C}''_l \\ -\frac{EA_s}{2} \left[\sum_{t=-2n}^{2n} \left(\sum_{q=-n}^{n} \vec{C}'_q \cdot \vec{C}'_{t-q}\right) \vec{C}'_{l-t}\right]', \quad for \ s = l \end{cases} \tag{2.40}$$

For s varying from *-3n* to *3n*, the total number of systems, like the preceding one (2.40), is *(6n+1)*. These systems are time independent and the resolution of the Fourier coefficients $\vec{C}_k$ can be carried out numerically.

- *With a hypothetical known force :*

  Another alternative is to consider a hypothetical known exciting force, which would have a simpler expression than the drag force.

  For a known forcing, i.e. $\vec{E}e^{ip\omega t}$, p is given and $\omega$ is the same as the $\omega$ of the motion considered defined by $\vec{r} = \sum_{k=-n}^{n} \vec{C}_k \ e^{in\omega t}$. Then, the response of the mooring line for this specific excitation force is given by :

$$\widetilde{M}\ddot{\vec{r}} - (\tilde{\lambda}\vec{r}')' = \vec{E}(s)e^{ip\omega t} \tag{2.41}$$

Under the assumption that the wave frequency $p\omega$ is a multiple of the slow-drift frequency $\omega$, the force $\vec{E}e^{ip\omega t}$ could model a fluid exciting force of frequency $p\omega$.

The more developed form of (2.41) is as follows :

$$\vec{E}e^{ip\omega t} = \begin{cases} -\left(\rho_s A_s + \rho_f A_f C_m\right)\omega^2 \sum_{s=-n}^{n} s^2 \vec{C}_s e^{is\omega t} \\ +\rho_f A_f C_m \omega^2 \sum_{s=-3n}^{3n} \left[\sum_{t=-2n}^{2n} \left(\sum_{q=-n}^{n} q^2 \vec{C}_q \cdot \vec{C}'_{t-q}\right) \vec{C}'_{s-t}\right] e^{is\omega t} \\ +\frac{EA_s}{2} \sum_{s=-n}^{n} \vec{C}''_s e^{is\omega t} \\ -\frac{EA_s}{2} \sum_{s=-3n}^{3n} \left[\sum_{t=-2n}^{2n} \left(\sum_{q=-n}^{n} \vec{C}'_q \cdot \vec{C}'_{t-q}\right) \vec{C}'_{s-t}\right]' e^{is\omega t} \end{cases} \tag{2.42}$$

with the constraint on the Fourier coefficients eq.(2.32).

Identification of the exponential terms on both sides of the equation leads to a system of non-linear equations where the unknowns are the coefficients $\vec{C}_k(s)$, $k = -n, ..., +n$, with the same condition eq.(2.32).

For $s = p$, the system becomes eq.(2.43) and for $-3n \leq s \leq 3n$ *and* $s \neq p$, the identification yields eq.(2.44).

$$\vec{E} = \begin{cases} -\left(\rho_s A_s + \rho_f A_f C_m\right)\omega^2 p^2 \vec{C}_p \\ +\rho_f A_f C_m \omega^2 \sum_{t=-2n}^{2n} \left(\sum_{q=-n}^{n} q^2 \vec{C}_q \cdot \vec{C}'_{t-q}\right) \vec{C}'_{p-t} \\ +\frac{EA_s}{2} \vec{C}''_p \\ -\frac{EA_s}{2} \left[\sum_{t=-2n}^{2n} \left(\sum_{q=-n}^{n} \vec{C}'_q \cdot \vec{C}'_{t-q}\right) \vec{C}'_{p-t}\right]' \end{cases} \tag{2.43}$$

$$\vec{0} = \begin{cases} -(\rho_s A_s + \rho_f A_f C_m)\,\omega^2 \sum_{s=-n}^{n} s^2\,\vec{C}_s e^{is\omega t} \\ +\rho_f A_f C_m\,\omega^2 \sum_{s=-3n}^{3n} \left[ \sum_{t=-2n}^{2n} \left( \sum_{q=-n}^{n} q^2\,\vec{C}_q \cdot \vec{C}'_{t-q} \right) \vec{C}'_{s-t} \right] e^{is\omega t} \\ +\frac{EA_s}{2} \sum_{s=-n}^{n} \vec{C}''_s e^{is\omega t} \\ -\frac{EA_s}{2} \sum_{s=-3n}^{3n} \left[ \sum_{t=-2n}^{2n} \left( \sum_{q=-n}^{n} \vec{C}'_q \cdot \vec{C}'_{t-q} \right) \vec{C}'_{s-t} \right]' e^{is\omega t} \end{cases} \tag{2.44}$$

For a given $s = l$, between *-3n* and *3n*, the second system of equations of eq.(2.44) leads to a system of vector equations of the form :

$$\vec{0} = \begin{cases} (\rho_s A_s + \rho_f A_f C_m)\,\omega^2 l^2\,\vec{C}_l \\ -\rho_f A_f C_m\,\omega^2 \left[ \sum_{t=-2n}^{2n} \left( \sum_{q=-n}^{n} q^2\,\vec{C}_q \cdot \vec{C}'_{t-q} \right) \vec{C}'_{l-t} \right] \\ +\frac{EA_s}{2}\,\vec{C}''_l \\ +\frac{EA_s}{2} \left[ \sum_{t=-2n}^{2n} \left( \sum_{q=-n}^{n} \vec{C}'_q \cdot \vec{C}'_{t-q} \right) \vec{C}'_{l-t} \right]', \quad for\ s = l \end{cases} \tag{2.45}$$

In this system, the *6n* vector equations are generated for each frequency. Overall, there are *(6n + 1)* vector equations.

Each of those equations leads to 3 equations, one for each physical dimension.

In this case, numerical solutions can be obtained for each Fourier coefficient $\vec{C}_k$ and therefore for the cable motion defined by $\vec{r}(s,t)$.

# CHAPTER 3

# CABLE CONFIGURATION

So far, in the mathematical formulation, no physical end conditions have been specified on the cable. However, without these conditions, the equation of motion can not be solved. This chapter defines a set of boundary conditions necessary to close the problem and then determines an analytical solution for the static case.

## 3.1 Graphical Representation

The cable has bottom and top boundary conditions. Along the cable the arclength $s$ is defined as $s = 0$ at the bottom of the line and $s = L$ at the top. The bottom point is fixed, allowing zero displacements. An imposed known force is applied at the top point of the cable, or the fairlead.

Graphically, these physical specifications are represented as shown in figure (3-1).

## 3.2 Boundary Conditions

The mathematical formulation of figure (3-1) can be expressed seperately for the static and the dynamic case according to the multiple scale theory and the Fourier decomposition.

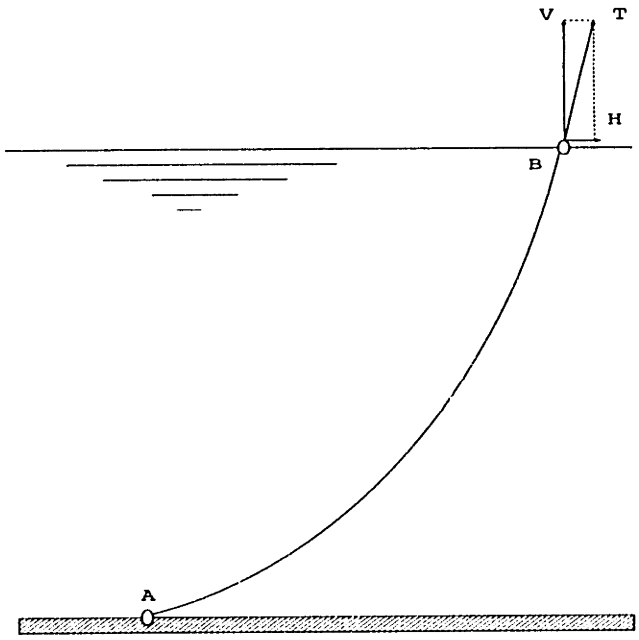


Figure 3-1: Cable Configuration

### 3.2.1 Static Case

The position vector $\vec{r}(s)$ is given by its two coordinates :

$$\vec{r}(s) = \vec{C}_o(s) = \begin{bmatrix} x(s) \\ z(s) \end{bmatrix}$$

and the derivative with respect to the arclength s is :

$$\frac{d\vec{r}}{ds} = \frac{d\vec{C}_o}{ds} = \begin{bmatrix} \frac{dx}{ds} \\ \\ \frac{dz}{ds} \end{bmatrix}$$

**Fixed bottom - imposed tension at the top**

The boundary conditions are then expressed as :

- $s = 0$ : *fixed point bottom*

$$\vec{r}(s) = \vec{0} \tag{3.1}$$

leading to

$$\vec{C}_o = \vec{0} \tag{3.2}$$

- $s = L$ : *imposed force at the top*

  - Continuity of the cable slope with the imposed force slope,

$$\begin{aligned} \tan\varphi &= \frac{V}{H} \\ &= \frac{dz/ds}{dx/ds} \end{aligned} \tag{3.3}$$

leading to

$$C'_{oz} = \frac{V}{H} C'_{ox} \tag{3.4}$$

  - Condition on the magnitude of the force applied at the top,

$$\begin{aligned} T &= \frac{EA_s}{2}\left(\vec{r}' \cdot \vec{r}' - 1\right) \\ T &= \sqrt{H^2 + V^2} \end{aligned} \tag{3.5}$$

leading to

$$\vec{C}'_o \cdot \vec{C}_o{}' = \frac{2}{EA_s}\sqrt{H^2 + V^2} + 1 \tag{3.6}$$

or, expressed with respect to the coordinates of $\vec{C}_o$,

$$C'^2_{ox} + C'^2_{oz} = \frac{2}{EA_s}\sqrt{H^2 + V^2} + 1 \tag{3.7}$$

The boundary conditions at the top of the cable are finally obtained from eq.(3.4) and eq.(3.7), yielding expressions (3.8) for $C'_{ox}$ and $C'_{oz}$.

$$\begin{cases} C'_{ox} &= \dfrac{H}{\sqrt{H^2+V^2}}\left(\dfrac{2}{EA_s}\sqrt{H^2+V^2}+1\right)^{\frac{1}{2}} \\ \\ C'_{oz} &= \dfrac{V}{\sqrt{H^2+V^2}}\left(\dfrac{2}{EA_s}\sqrt{H^2+V^2}+1\right)^{\frac{1}{2}} \end{cases} \tag{3.8}$$

### 3.2.2 Dynamic Case

The dynamic motion has the same bottom and top boundary conditions as the static motion. The position vector $\vec{r}_k(s,t)$ is given by its two coordinates, for a each frequency (k=1, 2).

$$\vec{r}(s,t) = \sum_{k=-n}^{+n} \vec{C}_k(s)\ e^{ik\omega t} = \begin{bmatrix} x(s) \\ z(s) \end{bmatrix}$$

Its derivative with respect to the arclength s is :

$$\frac{d\vec{r}}{ds} = \sum_{k=-n}^{+n} \frac{d\vec{C}_k(s)}{ds}\ e^{ik\omega t} = \sum_{k=-n}^{+n} \vec{C}'_k(s)\ e^{ik\omega t} = \begin{bmatrix} \dfrac{dx}{ds} \\ \\ \dfrac{dz}{ds} \end{bmatrix}$$

**Fixed bottom - imposed tension at the top**

The boundary conditions are then expressed as :

- *$s = 0$ : fixed point bottom*

$$\vec{r}_k(s,t) = \vec{0} \tag{3.9}$$

leading to

$$\vec{C}_k(s) = \vec{0}, \qquad k\text{=-}n,\ +n \tag{3.10}$$

- $s = L$ : *imposed force at the top*

  - Continuity of the cable slope with the imposed force slope,

$$\begin{aligned} \tan\varphi &= \frac{V}{H} \\ &= \frac{dz/ds}{dx/ds} \end{aligned} \tag{3.11}$$

Assuming the imposed force at the top can be decomposed into a Fourier series, similarly to the decomposition of $\vec{r}$, such that the excition force at the top oscillates hamonically :

$$T = \sum_{k=-b}^{+b} \vec{t_k}\, e^{ik\omega t} = \begin{bmatrix} H = \sum_{k=-b}^{+b} t_{kx}\, e^{ik\omega t} \\ \\ V = \sum_{k=-b}^{+b} t_{kz}\, e^{ik\omega t} \end{bmatrix}$$

Under this assumption, the condition (3.11) is given by :

$$\left(\sum_{k=-n}^{+n} C'_{kz}(s)\ e^{ik\omega t}\right)\cdot\left(\sum_{p=-b}^{+b} t_{px}\, e^{ip\omega t}\right) = \left(\sum_{k=-n}^{+n} C'_{kx}(s)\ e^{ik\omega t}\right)\cdot\left(\sum_{p=-b}^{+b} t_{pz}\, e^{ip\omega t}\right)$$

From eq.(A.3) and eq.(A.4), which consist of mathematical identities, given in appendix A, used to express the product of two series in a more compact way, the first boundary condition at the top leads to :

$$\sum_{l=-(n+b)}^{+(n+b)} \sum_{k=-b}^{+b} t_{kx}\, C'_{(l-k)z}\, e^{il\omega t} = \sum_{l=-(n+b)}^{+(n+b)} \sum_{k=-b}^{+b} t_{kz}\, C'_{(l-k)x}\, e^{il\omega t} \tag{3.12}$$

For $-(n+b) \leq l \leq +(n+b)$, identifying each exponential term yields the first condition at the top of the cable (3.13) :

$$\sum_{k=-b}^{+b} t_{kx}\, C'_{(l-k)z} \;=\; \sum_{k=-b}^{+b} t_{kz}\, C'_{(l-k)x} \tag{3.13}$$

– Condition on the magnitude of the force applied at the top,

$$\begin{aligned} T &= \frac{EA_s}{2}\left(\vec{r'}\cdot\vec{r'}-1\right) \\ T &= \sqrt{H^2+V^2} \end{aligned} \tag{3.14}$$

Recall that the imposed force is expressed by :

$$T = \sum_{k=-n}^{+n} \vec{t}_k\, e^{ik\omega t} = \begin{bmatrix} H = \sum_{k=-b}^{+b} t_{kx}\, e^{ik\omega t} \\ \\ V = \sum_{k=-b}^{+b} t_{kz}\, e^{ik\omega t} \end{bmatrix}$$

Therefore, the absolute value of the tension becomes :

$$T = \sqrt{\left(\sum_{k=-b}^{+b} t_{kx}\, e^{ik\omega t}\right)^2 + \left(\sum_{k=-b}^{+b} t_{kz}\, e^{ik\omega t}\right)^2} \tag{3.15}$$

Substituting for the expression of $(\vec{r'}\cdot\vec{r'})$, eq.(A.14) and eq.(A.15) from appendix A, in (3.14) yields :

$$\begin{aligned} &\sum_{p=-2n}^{2n}\left(\sum_{q=-n}^{n} \vec{C}'_q\cdot\vec{C}'_{p-q}\right) e^{ip\omega t} = \\ &\frac{2}{EA_s}\sqrt{\left(\sum_{k=-b}^{+b} t_{kx}\, e^{ik\omega t}\right)^2 + \left(\sum_{k=-b}^{+b} t_{kz}\, e^{ik\omega t}\right)^2} + 1 \end{aligned} \tag{3.16}$$

where $\vec{C}'_{p-q} = \vec{0}$ for $p-q > m$ and $p-q < -m$.

This condition can be expressed for each frequency, by identifying the exponential terms, only if certain assumptions are made concerning the nature of the imposed force at the top. In the case of a harmonic force applied in the horizontal direction, the vertical component of the tension, namely $t_{kz}$, is zero, therefore, the second boundary condition, at the fairlead, becomes:

$$\sum_{p=-2n}^{2n}\left(\sum_{q=-n}^{n}\vec{C}'_q\cdot\vec{C}'_{p-q}\right)e^{ip\omega t} = \frac{2}{EA_s}\left(\sum_{k=-b}^{+b}t_{kx}\,e^{ik\omega t}+1\right) \tag{3.17}$$

Identifying exponential terms, for each frequency, the boundary conditions are identified as follows:

* $p = k,\ p \neq 0\ and\ k \neq 0\ and\ -b \leq p \leq +b$

$$\sum_{q=-n}^{n}\vec{C}'_q\cdot\vec{C}'_{p-q} = \frac{2}{EA_s}t_{px} \tag{3.18}$$

* $p = k = 0$

$$\sum_{q=-n}^{n}\vec{C}'_q\cdot\vec{C}'_{-q} = \frac{2}{EA_s}(t_{ox}+1) \tag{3.19}$$

* $p \neq 0,\ p \neq k\ and\ -2n \leq p \leq +2n$

$$\sum_{q=-n}^{n}\vec{C}'_q\cdot\vec{C}'_{p-q} = 0 \tag{3.20}$$

For a vertically oscillating force, the equation for this boundary condition is defined by the expression (3.17) or by the set of equations (3.18), (3.19) and (3.20), where $t_x$ is replaced by $t_z$.

## 3.3 Analytical Solutions

For the static case, given the previously stated boundary conditions, analytical solutions can be easily derived for an inelastic or an elastic cable. These expressions

are chosen for the initialization of the static motion and permit the validation of the model for the static case. The derivation of such solutions is described in the following section.

### 3.3.1 Catenary Equations

These analytical solutions are found by solving the catenary equations which consist of the equations of equilibrium for a cable element. From these equations, the coordinates of the position vector, obtained geometrically, are solved and therefore the cable motion is determined.

**Equations of Equilibrium :**

$$\begin{cases} \dfrac{dT_e}{ds} = w_o \sin\varphi \\ T_e \dfrac{d\varphi}{ds} = w_o \cos\varphi \end{cases} \tag{3.21}$$

**Equations of Position :**

$$\begin{cases} \dfrac{dx}{ds} = (1+\epsilon)\cos\varphi \\ \dfrac{dz}{ds} = (1+\epsilon)\sin\varphi \end{cases} \tag{3.22}$$

where dx, dz and $\varphi$ are given by figure (3-2).

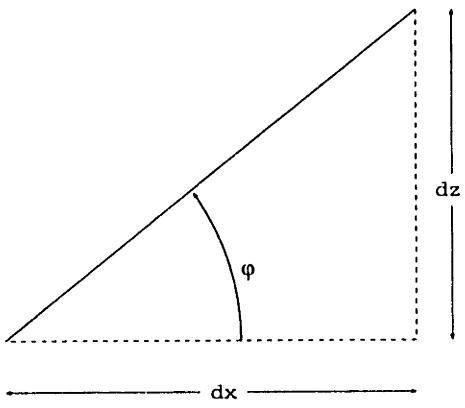


Figure 3-2: Definition of $\varphi$

**Behavioral Equation :**

$$\begin{cases} \epsilon = \dfrac{T_e}{E\,A_s} \\ \\ \quad = \dfrac{ds_1}{ds} - 1 \\ \\ T_e = T + P_e\,A_s \end{cases} \tag{3.23}$$

where $ds_1$ and $ds$ are, respectively, the infinitesinal segments of the cable of stretched and unstretched length.

### 3.3.2 Inelastic case

The position vector $\vec{r}(s)$ has two coordinates, one in the x- direction, $x(s)$, one in the z-direction, $z(s)$, and are found by solving the preceding catenary equations, where for the inelastic configuration, $\epsilon = 0$. Therefore, the displacements are given by :

$$\begin{cases} x = \dfrac{H}{w_o}\left(\ln\left|\dfrac{V - w_o(L-s)}{H} + \sqrt{1 + \left(\dfrac{V - w_o(L-s)}{H}\right)^2}\right|\right. \\ \\ \qquad \left. - \ln\left|\dfrac{V - w_oL}{H} + \sqrt{1 + \left(\dfrac{V - w_oL}{H}\right)^2}\right|\right) \\ \\ z = \dfrac{H}{w_o}\left(\sqrt{1 + \dfrac{V - w_o(L-s)^2}{H}} - \sqrt{1 + \dfrac{V - w_oL^2}{H}}\right) \end{cases} \tag{3.24}$$

and the tension is expressed by :

$$\begin{cases} T_e = \dfrac{H}{\cos\varphi} \\ \\ \quad = \sqrt{H^2 + [V - w_o(L-s)]^2} \\ \\ \tan\varphi = \dfrac{V}{H} - \dfrac{w_o}{H}(L-s) \end{cases} \tag{3.25}$$

The net weight of the cable in water per unit length is defined by :

$$w_o = (\rho_s A_s - \rho_f A_f)\ g \tag{3.26}$$

### 3.3.3 Elastic case

Solving the same catenary equations eq.(3.21), where $\epsilon \neq 0$, leads to the following displacements :

$$\begin{cases} x = \dfrac{H}{w_o}\left(\ln\left|\dfrac{V - w_o(L-s)}{H} + \sqrt{1 + \left(\dfrac{V - w_o(L-s)}{H}\right)^2}\right|\right. \\ \\ \quad \left. - \ln\left|\dfrac{V - w_o L}{H} + \sqrt{1 + \left(\dfrac{V - w_o L}{H}\right)^2}\right|\right) + \dfrac{Hs}{EA_s} \\ \\ z = \dfrac{H}{w_o}\left(\sqrt{1 + \left(\dfrac{V - w_o(L-s)}{H}\right)^2} - \sqrt{1 + \left(\dfrac{V - w_o L}{H}\right)^2}\right) \\ \\ \quad + \dfrac{1}{EA_s}\left(Vs - w_o\, s\,(L - \dfrac{s}{2})\right) \end{cases} \tag{3.27}$$

The tension $T_e$ and the weight $w_o$ are the same as in the inelastic case.

### Three Dimensional Generalization

The static problem can be solved in two dimensions, by chosing the adequate horizontal axis in the (x,y) plane, since the buoyancy effect and the weight of the cable are the only external forces on the mooring line.

The three dimensional problem is treated as described for a two dimensional case where $H = \sqrt{H_x^2 + H_y^2}$, $H_x$ and $H_y$ being the tension components in the x and y directions, respectively.

Let X and Z denote the two dimensional displacements expressed by eq.(3.24) for the inelastic case and eq.(3.27) for the elastic case, where X is the solution in the (x,y) plane and Z the solution in the z direction.

Therefore, the displacements in the x and y directions are given by :

$$\begin{cases} x = \dfrac{H_x}{\sqrt{H_x^2 + H_y^2}} X \\ \\ y = \dfrac{H_y}{\sqrt{H_x^2 + H_y^2}} X \end{cases} \tag{3.28}$$

The displacement in the z-direction Z is unchanged, since the gravity and the buoyancy both act in the vertical direction.

## 3.3.4 Comparison Between the Model and the Analytical Solution

As previously stated, the catenary equations (3.21) are as follows :

$$\begin{cases} \dfrac{dT_e}{ds} = w_o \sin\varphi \\ \\ T_e \dfrac{d\varphi}{ds} = w_o \cos\varphi \end{cases} \tag{3.29}$$

The rate of stretch along the cable is given by eq.(2.11) :

$$\vec{r'} = (1 + \frac{T_e}{EA_s})\vec{t} \tag{3.30}$$

where

$$\vec{t} = \begin{pmatrix} \cos\varphi \\ \sin\varphi \end{pmatrix} \tag{3.31}$$

The static equation of motion obtained in chapter two, given by eq.(2.19), is expressed as :

$$-(T_e\vec{r'})' = \vec{g}(\rho_f A_f - \rho_s A_s) \tag{3.32}$$

The restoring term $(T_e\vec{r'})'$ of the preceding equation can be determined in terms of expressions (3.21), (3.30), and (3.31) as follows :

$$\begin{aligned}(T_e\vec{r'})' = &\left[w_o \sin\varphi \left(1 + \frac{2w_o}{EA_s}\frac{1}{\varphi'}\cos\varphi\right)\right]\begin{bmatrix}\cos\varphi \\ \sin\varphi\end{bmatrix} \\ &+ \left[\frac{w_o\cos\varphi}{\varphi'}\left(1 + \frac{w_o}{EA_s}\frac{1}{\varphi'}\cos\varphi\right)\right]\begin{bmatrix}-\varphi'\sin\varphi \\ \varphi'\cos\varphi\end{bmatrix}\end{aligned} \tag{3.33}$$

Substituting the preceding expression (3.33) in the left hand side of eq.(2.19) yields that identity (3.34) should be verified.

$$
\begin{aligned}
(T_e\vec{r}')' &= \left[w_o \sin\varphi \left(1 + \frac{2w_o}{EA_s}\frac{1}{\varphi'}\cos\varphi\right)\right]\begin{bmatrix}\cos\varphi\\ \sin\varphi\end{bmatrix} \\
&\quad + \left[\frac{w_o\cos\varphi}{\varphi'}\left(1 + \frac{w_o}{EA_s}\frac{1}{\varphi'}\cos\varphi\right)\right]\begin{bmatrix}-\varphi'\sin\varphi\\ \varphi'\cos\varphi\end{bmatrix} \qquad (3.34)\\
&= -\vec{g}\,(\rho_f A_f - \rho_s A_s) \\
&= w_o\vec{e}_z
\end{aligned}
$$

where the net weight of the cable in water per unit length is defined by :

$$w_o = (\rho_s\, A_s - \rho_f\, A_f)\; g \qquad (3.35)$$

However this identity can not be satisfied unless the following assumption is made:

$$\frac{w_o}{EA_s}\frac{\cos\varphi}{\varphi'} \ll 1 \qquad (3.36)$$

It is therefore concluded that the model is expected to agree with the analytical solution of the catenary equations when the above assumption (3.36) is valid.

# CHAPTER 4

# NUMERICAL IMPLEMENTATION

Once the mathematical and physical problems have been completely determined, the numerical implementation of this formulation presents a few aspects which need to be discussed.

The goal of the numerical implementation is to discretize the equation of motion and boundary conditions. As a result, a system of non-linear difference equations will be obtained. The Newton-Raphson method used to solve these equations is discussed in this chapter. Finally, several initial guesses for the cable configuration, necessary to start the iterative Newton-Raphson procedure, are expressed.

## 4.1 Discretization

The cable has been divided into *N-1* total elements from $s = 0$ to $s = L$. The nodes are labelled from *1* to *N*. The element length is obtained by dividing the total length of the cable by the number of elements, $\Delta s = \frac{L}{N-1}$. The arclength, s, is incremented by $\Delta s$, $s = (IE - 1)\,\Delta s$, where *IE* is the node counter and ranges from *1* to *N*, such that $s$ ranges from *0* to $L$.

### 4.1.1 Static Case

#### Form for the equation of motion

The static problem is a two-dimensional problem. Since the cable is divided into *N-1* elements, the static equations of motion eq.(2.21) and eq.(2.22) lead to a system of *2(N-1)* non-linear equations. These equations can be solved using a multidimensional rootfinding method.

#### First and second derivative schemes :

The equation of motion as well as the boundary conditions involve first and second derivatives of the Fourier coefficient, $\vec{C}_o$, and derivatives of more complex expressions depending on this $\vec{C}_o$. Therefore, discretization schemes are required for the numerical implementation process.

At the top, the first and second derivatives have been modeled by a backward finite difference scheme while at the bottom, a forward scheme was used. Between the first and last element of the cable, the derivatives have been modeled using the centered finite difference scheme.

#### At the bottom of the cable, s = 0:

- *First order scheme :*

$$\vec{C}_o'(s) = \frac{\vec{C}_o(\Delta s) - \vec{C}_o(0)}{\Delta s} \tag{4.1}$$

- *Second order scheme :*

$$\begin{cases} \vec{C}_o'(s) = \dfrac{1}{2\,\Delta s}\left(-3\,\vec{C}_o(0) + 4\,\vec{C}_o(\Delta s) - \vec{C}_o(2\,\Delta s)\right) \\ \\ \vec{C}_o''(s) = \dfrac{1}{\Delta s^2}\left(\vec{C}_o(2\Delta s) - 2\,\vec{C}_o(\Delta s) + \vec{C}_o(0)\right) \end{cases} \tag{4.2}$$

**At the top of the cable, s = L:**

- *First order scheme :*

$$\vec{C}_o'(s) = \frac{\vec{C}_o(L) - \vec{C}_o(L - \Delta s)}{\Delta s} \tag{4.3}$$

- *Second order scheme :*

$$\begin{cases} \vec{C}_o'(s) = \dfrac{1}{2\,\Delta s}\left(-3\,\vec{C}_o(L) - 4\,\vec{C}_o(L - \Delta s) + \vec{C}_o(L - 2\,\Delta s)\right) \\ \\ \vec{C}_o''(s) = \dfrac{1}{\Delta s^2}\left(\vec{C}_o(L - 2\,\Delta s) - 2\,\vec{C}_o(L - \Delta s) + \vec{C}_o'(L)\right) \end{cases} \tag{4.4}$$

**For $0 < s < L$:**

- *Second order scheme :*

$$\begin{cases} \vec{C}_o'(s) = \dfrac{\vec{C}_o(s + \Delta s) - \vec{C}_o(s - \Delta s)}{2\Delta s} \\ \\ \vec{C}_o''(s) = \dfrac{1}{\Delta s^2}\left(\vec{C}_o(s + \Delta s) + \vec{C}_o(s - \Delta s) - 2\,\vec{C}_o(s)\right) \end{cases} \tag{4.5}$$

- *Fourth order scheme :*

$$\begin{aligned} \vec{C}_o'(s) = \frac{1}{12\Delta s}\big(&\vec{C}_o(s - 2\,\Delta s) - 8\,\vec{C}_o(s - \Delta s) \\ &+8\,\vec{C}_o(s + \Delta s) - \vec{C}_o(s + 2\,\Delta s)\big) \end{aligned} \tag{4.6}$$

**Discretization of $\left[\left(\vec{C}_o' \cdot \vec{C}_o'\right)\vec{C}_o'\right]'$:**

The terms $\left(\left(\vec{C}_o' \cdot \vec{C}_o'\right) C_o'\right)_x'$ and $\left(\left(\vec{C}_o' \cdot \vec{C}_o'\right) C_o'\right)_z'$ in the static system of equations of motion eq.(2.21) and eq.(2.22), have been modeled for $s = 0$, $0 < s < L$ and $s = L$.

- *At* $s = 0$ :

$$\begin{cases} \left(\left(\vec{C}_o' \cdot \vec{C}_o'\right) C_o'\right)_x' = \frac{1}{\Delta s}\left[C_{ox}(\Delta s)\left(C_{ox}^2(\Delta s) + C_{oz}^2(\Delta s)\right)\right. \\ \qquad\qquad \left. - C_{ox}(0)\left(C_{ox}^2(0) + C_{oz}^2(0)\right)\right] \\ \left(\left(\vec{C}_o' \cdot \vec{C}_o'\right) C_o'\right)_z' = \frac{1}{\Delta s}\left[C_{oz}(\Delta s)\left(C_{ox}^2(\Delta s) + C_{oz}^2(\Delta s)\right)\right. \\ \qquad\qquad \left. - C_{oz}(0)\left(C_{ox}^2(0) + C_{oz}^2(0)\right)\right] \end{cases}$$

- *At* $s = L$ :

$$\begin{cases} \left(\left(\vec{C}_o' \cdot \vec{C}_o'\right) C_o'\right)_x' = \frac{1}{\Delta s}\left[C_{ox}(L)\left(C_{ox}^2(L) + C_{oz}^2(L)\right)\right. \\ \qquad\qquad \left. - C_{ox}(L-\Delta s)\left(C_{ox}^2(L-\Delta s) + C_{oz}^2(L-\Delta s)\right)\right] \\ \left(\left(\vec{C}_o' \cdot \vec{C}_o'\right) C_o'\right)_z' = \frac{1}{\Delta s}\left[C_{oz}(L)\left(C_{ox}^2(L) + C_{oz}^2(L)\right)\right. \\ \qquad\qquad \left. - C_{oz}(L-\Delta s)\left(C_{ox}^2(L-\Delta s) + C_{oz}^2(L-\Delta s)\right)\right] \end{cases}$$

- *For* $0 < s < L$ :

$$\begin{cases} \left(\left(\vec{C}_o' \cdot \vec{C}_o'\right) C_o'\right)_x' = \frac{1}{2\Delta s}\left[C_{ox}(s+\Delta s)\left(C_{ox}^2(s+\Delta s) + C_{oz}^2(s+\Delta s)\right)\right. \\ \qquad\qquad \left. - C_{ox}(s-\Delta s)\left(C_{ox}^2(s-\Delta s) + C_{oz}^2(s-\Delta s)\right)\right] \\ \left(\left(\vec{C}_o' \cdot \vec{C}_o'\right) C_o'\right)_z' = \frac{1}{2\Delta s}\left[C_{oz}(s+\Delta s)\left(C_{ox}^2(s+\Delta s) + C_{oz}^2(s+\Delta s)\right)\right. \\ \qquad\qquad \left. - C_{oz}(s-\Delta s)\left(C_{ox}^2(s-\Delta s) + C_{oz}^2(s-\Delta s)\right)\right] \end{cases}$$

### 4.1.2 Dynamic Case

#### Form for the equation of motion

From the decomposition of the cable into a number of elements *(N-1)*, over its total length, and given that the Fourier coefficients $\vec{C}_k$ are complex, that the problem has three dimensions, and that there are *(6n+1)* systems of equations for each frequency, the total number of equations in this problem ends up being *6 (6n+1) (N-1).*

The discretized equations obtained from eq.(2.40) can be written as a multidimensional rootfinding problem for the $i^{th}$ element of the cable and for the $n^{th}$ exponential term.

#### First and second derivative schemes :

The dynamic equation of motion and boundary conditions also have first and second derivatives of the Fourier coefficients, $\vec{C}_k$, and derivatives of more complex expressions depending on these $\vec{C}_k$, to discretize. The finite difference schemes used for the dynamic case are similar to those described in for the static case for $s = 0$, $0 < s < L$ and $s = L$, with the index 'o' replaced by the corresponding index since there are multiple Fourier coefficients $\vec{C}_k$, $k = -n, ..., +n$, in the dynamic case.

#### Discretization of $\left[\left(\vec{C}'_q \cdot \vec{C}'_{t-q}\right) \vec{C}'_{l-t}\right]'$:

In the dynamic system of equations of motion, the terms $\left[\left(\vec{C}'_q \cdot \vec{C}'_{t-q}\right) C'_{l-t}\right]'_x$ and $\left[\left(\vec{C}'_q \cdot \vec{C}'_{t-q}\right) C'_{l-t}\right]'_z$ have been modeled for $s = 0$, $0 < s < L$ and $s = L$.

- *At $s = 0$ :*

$$\begin{cases} \left[\left(\vec{C}'_q \cdot \vec{C}'_{t-q}\right) C'_{l-t}\right]'_x = \frac{1}{\Delta s}\left[C'_{(l-t)x}(\Delta s)\left(C'_{qx}(\Delta s) \cdot C'_{(t-q)x}(\Delta s)\right.\right. \\ \qquad\qquad +C'_{qz}(\Delta s) \cdot C'_{(t-q)z}(\Delta s)\Big) \\ \qquad\qquad -C'_{(l-t)x}(0)\left(C'_{qx}(0) \cdot C'_{(t-q)x}(0) + C'_{qz}(0) \cdot C'_{(t-q)z}(0)\right)\Big] \\ \left[\left(\vec{C}'_q \cdot \vec{C}'_{t-q}\right) C'_{l-t}\right]'_z = \frac{1}{\Delta s}\left[C'_{(l-t)z}(\Delta s)\left(C'_{qx}(\Delta s) \cdot C'_{(t-q)x}(\Delta s)\right.\right. \\ \qquad\qquad +C'_{qz}(\Delta s) \cdot C'_{(t-q)z}(\Delta s)\Big) \\ \qquad\qquad -C'_{(l-t)z}(0)\left(C'_{qx}(0) \cdot C'_{(t-q)x}(0) + C'_{qz}(0) \cdot C'_{(t-q)z}(0)\right)\Big] \end{cases}$$

- *At $s = L$ :*

$$\begin{cases} \left[\left(\vec{C}'_q \cdot \vec{C}'_{t-q}\right) C'_{l-t}\right]'_x = \frac{1}{\Delta s}\left[C'_{(l-t)x}(L)\left(C'_{qx}(L) \cdot C'_{(t-q)x}(L) + C'_{qz}(L) \cdot C'_{(t-q)z}(L)\right)\right. \\ \qquad\qquad -C'_{(l-t)x}(L-\Delta s)\left(C'_{qx}(L-\Delta s) \cdot C'_{(t-q)x}(L-\Delta s)\right. \\ \qquad\qquad \left.+C'_{qz}(L-\Delta s) \cdot C'_{(t-q)z}(L-\Delta s)\right)\Big] \\ \left[\left(\vec{C}'_q \cdot \vec{C}'_{t-q}\right) C'_{l-t}\right]'_z = \frac{1}{\Delta s}\left[C'_{(l-t)z}(L)\left(C'_{qx}(L) \cdot C'_{(t-q)x}(L) + C'_{qz}(L) \cdot C'_{(t-q)z}(L)\right)\right. \\ \qquad\qquad -C'_{(l-t)z}(L-\Delta s)\left(C'_{qx}(L-\Delta s) \cdot C'_{(t-q)x}(L-\Delta s)\right. \\ \qquad\qquad \left.+C'_{qz}(L-\Delta s) \cdot C'_{(t-q)z}(L-\Delta s)\right)\Big] \end{cases}$$

- *For* $0 < s < L$ :

$$
\begin{cases}
\left[\left(\vec{C}'_q \cdot \vec{C}'_{l-q}\right) C'_{l-t}\right]'_x &= \frac{1}{2\Delta s}\left[C'_{(l-t)x}(s+\Delta s)\left(C'_{qx}(s+\Delta s)\cdot C'_{(t-q)x}(s+\Delta s)\right.\right. \\
&\quad \left. +C'_{qz}(s+\Delta s)\cdot C'_{(t-q)z}(s+\Delta s)\right) \\
&\quad -C'_{(l-t)x}(s-\Delta s)\left(C'_{qx}(s-\Delta s)\cdot C'_{(t-q)x}(s-\Delta s)\right. \\
&\quad \left.\left. +C'_{qz}(s-\Delta s)\cdot C'_{(t-q)z}(s-\Delta s)\right)\right] \\
\left[\left(\vec{C}'_q \cdot \vec{C}'_{l-q}\right) C'_{l-t}\right]'_z &= \frac{1}{2\Delta s}\left[C'_{(l-t)z}(s+\Delta s)\left(C'_{qx}(s+\Delta s)\cdot C'_{(t-q)x}(s+\Delta s)\right.\right. \\
&\quad \left. +C'_{qz}(s+\Delta s)\cdot C'_{(t-q)z}(s+\Delta s)\right) \\
&\quad -C'_{(l-t)z}(s-\Delta s)\left(C'_{qx}(s-\Delta s)\cdot C'_{(t-q)x}(s-\Delta s)\right. \\
&\quad \left.\left. +C'_{qz}(s-\Delta s)\cdot C'_{(t-q)z}(s-\Delta s)\right)\right]
\end{cases}
$$

## 4.2 Newton-Raphson Method

Consider the two dimensional case, where the following equations need to be solved simultaneously :

$$
\begin{cases}
f(x,y) &= 0 \\
g(x,y) &= 0
\end{cases}
\tag{4.7}
$$

The functions f and g are two arbitrary functions, each of which has zero contour lines that divide the (x,y) plane into regions where their respective function is positive or negative. These zero contour boundaries are of interest in the rootfinding problem.

The solutions are the points which are common to the zero contours of f and g.

Unfortunately, the functions f and g, generally, have no relation to each other. Therefore, in order to find all common points, which are the solutions of the non-linear equations, the full zero contours of both functions need to be found. In addition, the zero contours will, in general, consist of an unknown number of disjoint closed curves. For more than two dimensions, the problem is to find points mutually common to *N* unrelated zero contours planes, each of dimensions *(N-1)*, which is an extremely complicated problem.

For non-linear systems of equations with more than two dimensions, the rootfinding problem is very complex to solve. However, once you identify the neighborhood of a root, or of a region where there might be a root, then the problem can be solved using the Newton-Raphson method which can be generalized to multiple dimensions. This method gives a very efficient means of converging to the root, providing that the initial guess is not too far from an existing root.

The equations, for both the static and the dynamic cases, give *N* functional relations involving variables $x_i$, $i$=-*N*,...,*N*.

Denote $\vec{X}$ the entire vector of values $x_i$, then in the neighborhood of $\vec{X}$, each of the functions $f_i$ can be expanded in Taylor series :

$$f_i(\vec{X} + \delta\vec{X}) = f_i(\vec{X}) + \sum_{j=1}^{N} \frac{\partial f_i}{\partial x_j} \delta x_j + \mathcal{O}(\delta\vec{X}^2) \tag{4.8}$$

By neglecting the terms of order $\delta\vec{X}^2$ and higher, a set of non-linear equations for the correction $\delta\vec{X}$ that move each function closer to zero simultaneously is obtained.

This system of non-linear equations is given by :

$$\sum_{j=1}^{N} \alpha_{ij}\, \delta x_j = \beta_i \tag{4.9}$$

where

$$\begin{cases} \alpha_{ij} \equiv \dfrac{\partial f_i}{\partial x_j} \\ \\ \beta_i \equiv -f_i \end{cases} \tag{4.10}$$

Matrix equation (4.9) can be solved by LU decomposition. The solution vector is then given by :

$$x_i^{new} = x_i^{old} + \delta x_i, \quad \text{i=1,...,N} \tag{4.11}$$

and the process is iterated to convergence. Further details about the method can be found in *Numerical Analysis* [1] and *Numerical Recipes* [7].

## 4.3 Initial Guess

The method described above eq.(4.11) requires the initialization of $x_i^{old}$ in order to start the iterative process. For both the static and the dynamic cases, several options are described in the following sections.

### 4.3.1 Static Case

For the static case, the cable configuration is chosen to be initialized by the analytical solutions derived in the preceding chapter for an inelastic cable eq.(3.24) or an elastic cable eq.(3.27).

### 4.3.2 Dynamic Case

For the dynamic case, one intial guess consists of the resulting displacements of the static case and is the most natural initialization for the dynamic motion of the cable. From the multiple scale decomposition $\vec{r} = \vec{r}_o + \vec{r}_1 + \vec{r}_2$, where $\vec{r}_o$ describes the static motion, $\vec{r}_1$ describes the wave frequency motion and $\vec{r}_2$ describes the slow-drift motion,

the initial guess would then be expressed by (4.12).

$$\begin{cases} \vec{r}_o = \vec{C}_o & ,\vec{C}_o \text{ known} \\ \vec{r}_1 = \vec{0} \\ \vec{r}_2 = \vec{0} \end{cases} \tag{4.12}$$

This is the initial guess used in the numerical simulations presented in the next chapter.

# CHAPTER 5

# NUMERICAL RESULTS

Some tests of the numerical implementation described in the previous chapter have been performed. For the static case, the main goal was to validate the multiple scale model by comparing the simulated displacements of a basis line configuration with analytical solutions, and by conducting convergence tests with increasing number of elements along the cable. For the dynamic case, the wave frequency motion and the slow-drift motion have been investigated. Convergence tests are presented for the displacement of the cable, for these two modes of motion, at one given time. Snapshots of the cable motion for the wave frequency and the slow-drift motions are presented over half of period in order to visualize the displacements in time. For both the validation of the static model and for the analysis of the dynamic motions, two different types of cable material, steel and synthetic, have been investigated.

## 5.1 Static Motion

### 5.1.1 Basis Case

A basis case is used in the static simulations in order to validate the model. The physical characteristics of the cable and the fluid for the basis case are given in table (5.1). The force imposed at the top of the cable has a horizontal and vertical

component given in the same table (5.1) and the bottom point is fixed. Both steel and synthetic cables are considered.

| | |
|---|---|
| cable density for steel$(kg/m^3) = \rho_s$ | 7000 |
| cable density for synthetic $(kg/m^3) = \rho_s$ | 2000 |
| horizontal component of tension $(N) = H$ | 4,000 |
| vertical component of tension $(N) = V$ | 8,000 |
| Young's modulus $(N/m^2) = E$ | $10^9$ |
| structural cross sectional area $(m^2) = A_s$ | $2 \cdot 10^{-4}$ |
| cable length (m) = L | 600 |
| gravity $(m/s^2)$ = g | 9.81 |
| fluid density $(kg/m^3) = \rho_f$ | 1000 |
| cross sectional area for added mass $(m^2) = A_f$ | $2 \cdot 10^{-4}$ |

Table 5.1: Material properties - basis case

### 5.1.2 Validation of Model

Once the basic case parameters are determined, numerical simulations are performed. Some numerical characteristics are given in table (5.2).

Different densities, varying from $2,000\, Kg/m^3$ for synthetic cables such as nylon, to $7,000\, Kg/m^3$ for steel, are used in order to compare the mechanical behavior of the mooring line for different materials, which have various elastic elongations.

The static problem can be treated as a two-dimensional problem. The equations solved are the ones derived in chapter two. The simulated results are compared with the analytical solutions, defined in chapter three. The total number of elements

| | |
|---|---|
| total number of elements of the cable | (N-1) |
| number of dimensions | 2 |
| maximum number of iterations for the Newton-Raphson method | 20 |
| length of an element $\Delta s$ | $\frac{L}{N-1}$ |

Table 5.2: Numerical parameters used in the simulations

along the cable has been varied in order to demonstrate convergence of the model with respect to the theoretical displacements. The length of an element varies as a function of the total number of elements on the cable. In the simulations, the selected number of elements are five, ten and one hundred and fifty, such that the length of one element is provided in table (5.3).

| N-1 | 5 | 10 | 150 |
|---|---|---|---|
| $\Delta s$ $(m)$ | 120 | 60 | 4 |

Table 5.3: Length of a cable element for various number of elements

Figure (5-1) shows convergence of the static displacements for a steel cable with an increasing number of elements to the theoretical displacements given by (3.27) in chapter three, while figure (5-2) displays the tension calculated in the simulations compared to the theoretical expression (3.25) derived from the catenary equations. The tension is plotted against the curvilinear coordinate $s$, going from the anchor at $s = 0$ to the fairlead at $s = L$.

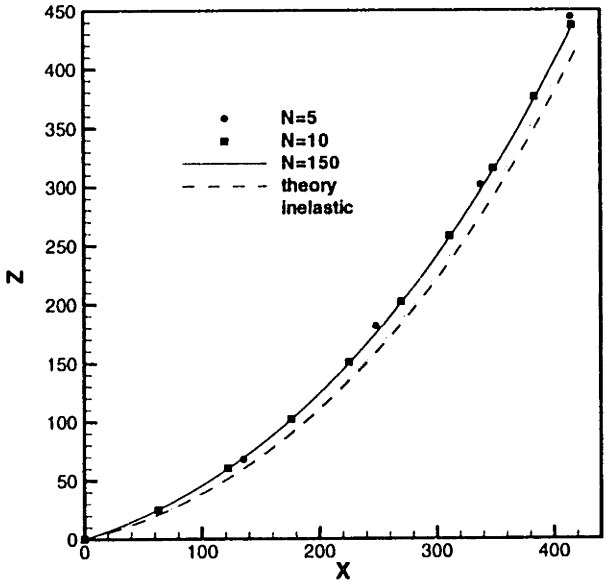


Figure 5-1: Convergence of the displacements for a steel cable and comparison to the analytical static solution

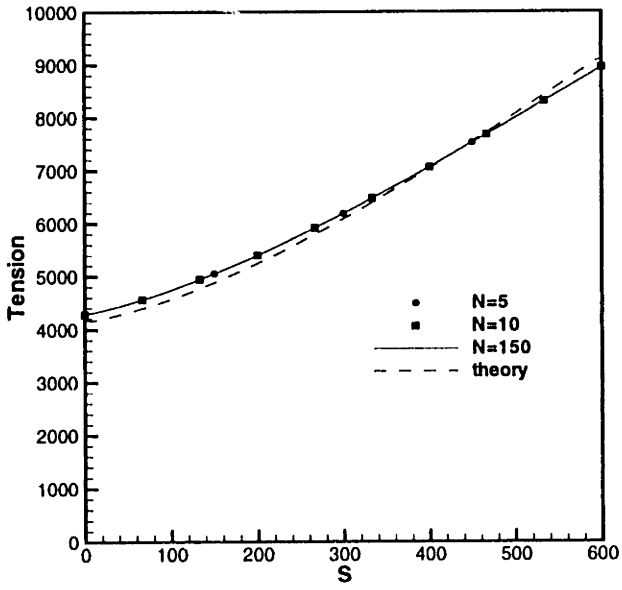


Figure 5-2: Convergence of the tension for a steel cable and comparison to the analytical static solution

For the displacements, convergence from five to one hundred and fifty elements is quite instantaneous accoring to the preceding figure (5-1). However, the asymptotic limit reached by the numerical results differs slightly from the static theoretical solution (3.27) obtained in chapter three.

Similar observations are made for the tension. The runs tend to a limit curve when the number of elements varies from five to ten and finally to one hundred and fifty elements. Only a small difference is observable between the exact and the approximated predictions.

Figure (5-3) illustrates convergence of displacement for a synthetic cable with increasing number of elements for a synthetic cable. Figure (5-4) compares the tension as a function of the arc length $s$ for the above simulations to the theoretical value.

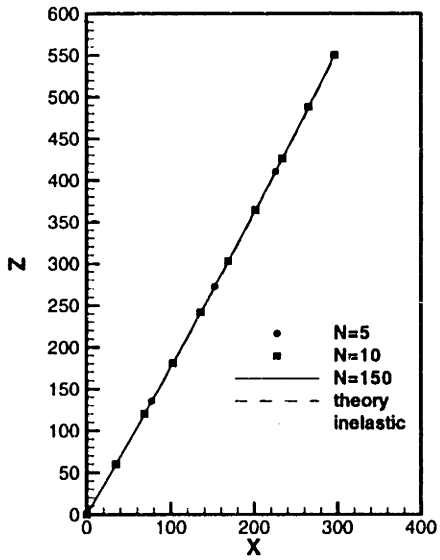


Figure 5-3: Convergence of the displacements for a synthetic cable and comparison to the analytical static solution

For a low number of elements, the results of the simulations are already close to the theoretical values. When increasing the numbers of elements up to one hundred and fifty, the gap bewteen the two vanishes. The numerically computed tension reaches an asymptotic curve sligthly different from the theory.

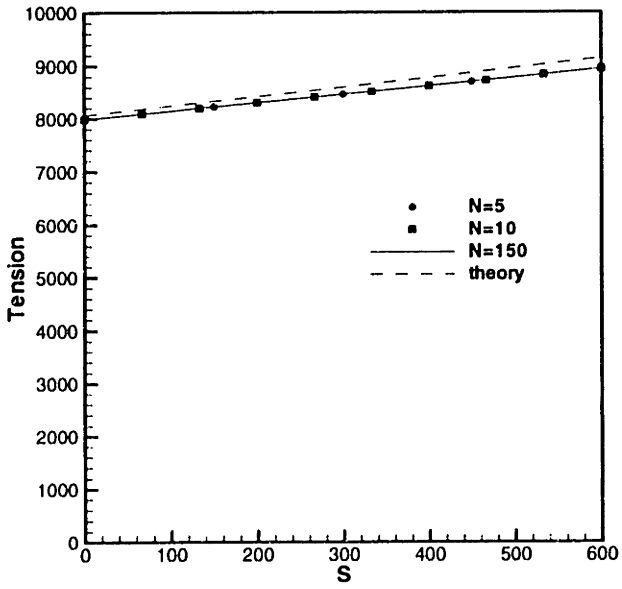


Figure 5-4: Convergence of the tension for a synthetic cable and comparison to the analytical static solution

The small discrepancies observed in figures (5-1), (5-2) and (5-4) is due to the assumption made by the model in the expression of the equations of motion for the static case described in chapter two. Since both the vector position $\vec{r}$ and the tension $T_e$ depend on the resolution of this equation, both the cable displacement and the tension are affected by this hypothesis. This approximation consists of a slight simplification concerning the restoring term $(T_e\vec{r}')'$ of eq.(2.19). As shown in section 3.3.4, the model agrees with the analytical solution only if the following condition, eq.(3.36), is satisfied :

$$\frac{w_o}{EA_s}\frac{\cos\varphi}{\varphi'} \ll 1 \tag{5.1}$$

where

$$\tan\varphi = \frac{V}{H} - \frac{w_o}{H}(L-s) \tag{5.2}$$

Moreover, the modeled tension, given by eq.(2.14), is not an exact expression either. The assumption that $\epsilon = \dfrac{T_e}{EA_s} \ll 1$ has been made in order to obtain an expression for the tension $T_e$. Therefore, these two assumptions influence the

simulated cable displacement and tension.

Values of $\frac{w_o}{EA_s}\frac{\cos\varphi}{\varphi'}$ along the line from $s = 0$ to $s = L$ for synthetic were found to be lower than the values for steel. As a result, the discrepancy between the model and the analytical solution is smaller than for the steel cable. In fact, there is no visible difference in displacements, but even the slightest gap is amplified for the tension calculation, so a difference was still observed in figure (5-4).

As expected, the higher the number of elements, the more accurate the rootfinding method becomes and therefore, the closer the numerical results are to the analytical solutions. Convergence is reached faster for the synthetic cable because larger elastic elongations of the cable are easier to be handled numerically by the model.

Overall, the convergence of the model to theory has been verified for increasing numbers of elements along the line. The converged results are also very close to the analytical predictions. Therefore, the conclusion of these simulations for the static basis case is that the model based on the multiple scale theory and the Fourier analysis of the equation of motion, detailed in chapter two, has been validated for the static component for steel and synthetic materials.

## 5.2 Dynamic Motion

For the dynamic case, similar tests were performed. In addition to varying the number of elements along the mooring line, in order to prove convergence of the approximated solution, other parameters of the problems have been investigated. First of all, both the wave frequency induced motion and the slow-drift frequency motion can be taken into account in the simulations. Second, the nature of the imposed force on the top of the line can either be harmonically oscillating in an horizontal or vertical manner. The convergence tests are carried out for a given time, chosen to be $t=0$, while snapshots of the cable configuration are displayed for both excitation frequencies, over half a period, representing the time variation of the cable motion. For both dynamic motions, two different materials have been tested and compared. For the convergence test runs, the number of elements was varied from ten to fourty. The basic material

and fluid properties are found in table (5.1), defined for the static case.

### 5.2.1 Wave Frequency

The wave frequency component is a small amplitude and quickly varying time dependent motion. The wave frequency which has been investigated corresponds to a relatively long wave period and wave length. In addition to the static force component, a harmonic force is imposed at the fairlead. This time dependent component varies first horizontally and then vertically, such that : $F_{top} = A\cos(\omega t + \Phi)$, where A is the magnitude of the oscillating force and $\Phi$ is the phase difference between the force and the cable motion. The magnitude of the force is fixed to *300 N* for all runs, but can be varied in order to model different boundary conditions at the fairlead. The phase is chosen to be zero. The test case is simulated for wave periods of $T =$ *10 s* and its wave characteristics are provided in table (5.4).

| | | |
|---|---|---|
| Wave period $T$ | $=$ | 10 $s$ |
| Wave frequency $\omega$ | $\approx$ | 0.63 $rad/s$ |
| Wave length $\lambda$ | $\approx$ | 155 $m$ |

Table 5.4: Wave frequency properties

#### Convergence

Figures (5-5) and (5-6) show the wave frequency motion, at a time $t = 0$, for waves of $T = 10$ $s$, respectively for a steel and a synthetic cable. The number of elements, denoted by N on the plots, has been varied from ten to fourty in order to prove convergence.

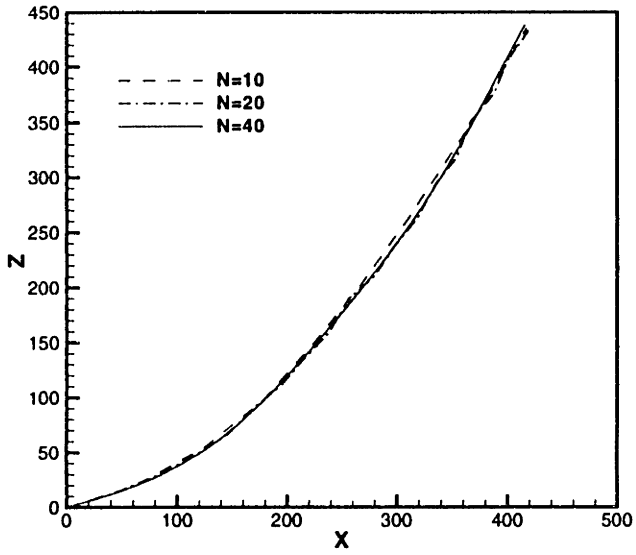


Figure 5-5: Convergence for wave period of $T = 10\ s$ for a steel cable

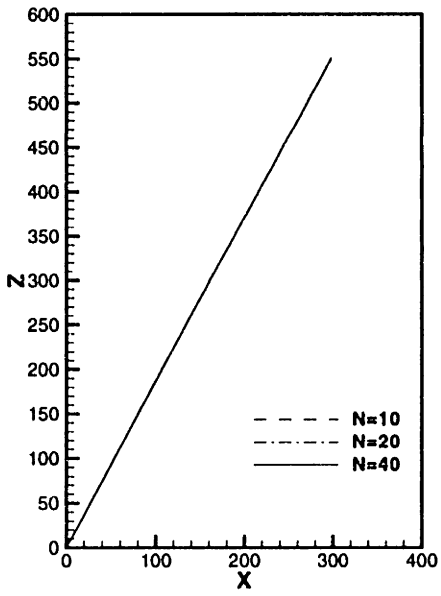


Figure 5-6: Convergence for wave period of $T = 10\ s$ for a synthetic cable

The wave frequency displacement easily tends to a converged limit with increasing number of elements. In fact, small variations in the cable displacement are observed when ranging elements from ten to twenty and finally to fourty, especially for a synthetic material. The lighter cable undergoing high tensions at both ends, due to the fixed bottom and the imposed force at the top, behaves like a string and adopts a linear shape as a result. The heavier cable tends to a more catenary shape form, since its weight acts against the imposed tension at the fairlead.

### Cable Motion

Once the equations for the Fourier coefficients $\vec{C}_k$ have been numerically solved, the vector position defined by $\vec{r}(s,t) = \sum_{k=-n}^{n} \vec{C}_k(s)\ e^{ik\omega t}$ is determined, for a given time t, by summing the $\vec{C}_k$ in the previous expression. Snapshots of the cable shape are then available and the superposition of these snapshots illustrates the wave frequency dynamic motion of the cable. For fourty elements and for a wave period of $T = 10\ s$, snapshots for five equally distributed times over half a period, have been produced, so that the cable motion can be viewed in time. The force at the fairlead is first oscillating horizontally and then vertically. The result of the cable motion is illustrated in figure (5-7), for a horizontal force and a steel cable, in figure (5-8) for the same forcing direction but a synthetic cable, in figure (5-9) for a vertical force and a steel cable and in figure (5-10) for a synthetic cable again under a vertical force.

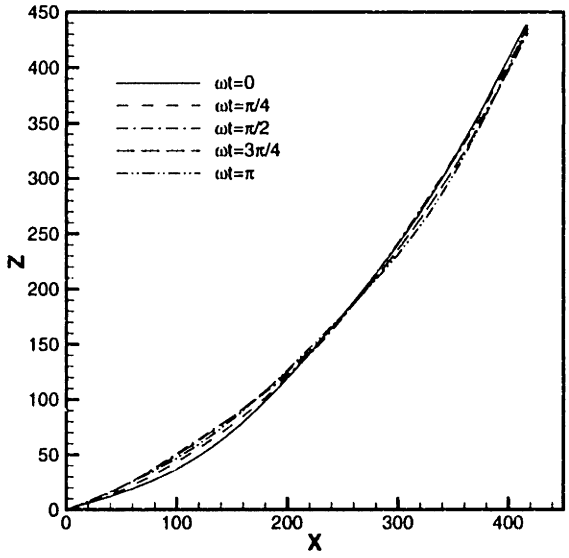


Figure 5-7: Wave frequency motion under horizontally oscillating force for a steel cable

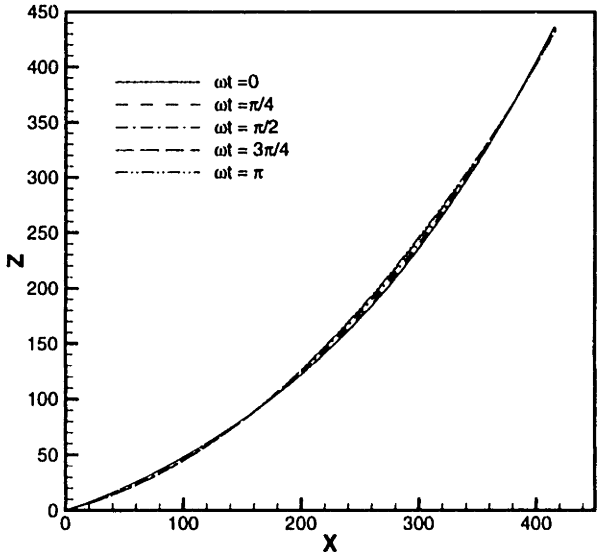


Figure 5-8: Wave frequency motion under vertically oscillating force for a steel cable

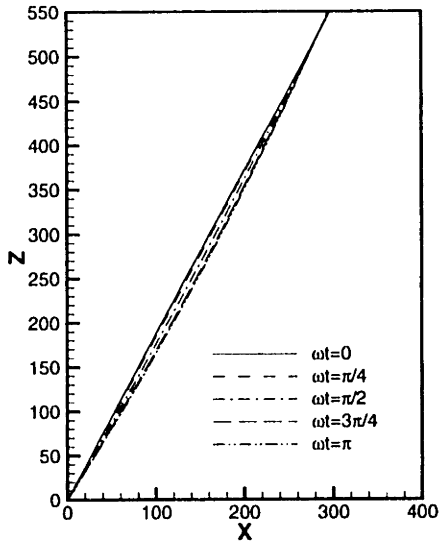


Figure 5-9: Wave frequency motion under horizontally oscillating force for a synthetic cable

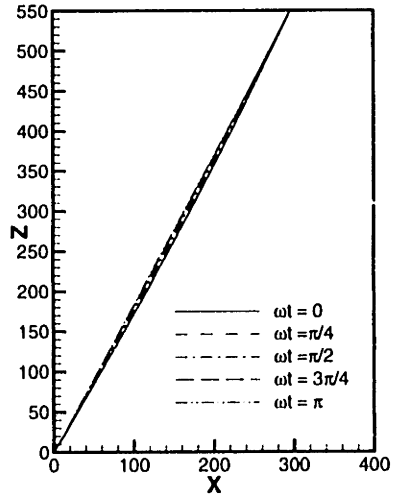


Figure 5-10: Wave frequency motion under horizontally oscillating force for a synthetic cable

The harmonic oscillation over half a period is shown in figures (5-7), (5-8), (5-9) and (5-10). The two materials display a different response to the time dependent forcing. The heavier cable oscillates in a hybrid second mode, while the ligther one oscillates in a first mode of motion. This characteristic can only be predicted with a fully dynamic method. For a vertically oscillating force at the top of the line, the displacements of a synthetic cable are reduced compared to the displacements due to a horizontal excitation but still oscillates in the same mode. However, as can be expected, the vertical force induces higher (lower) displacements in the $z$ ($x$) direction for $\omega t = \pi$ whereas the maximum (minimum) displacements in the $z$ ($x$) direction occurs for $\omega t = 0$ for a horizontal force. For a steel cable, the vertical excitation induces a third hybrid mode of motion, different in shape and with a lower magnitude than the case where the excitation is horizontally oscillating.

### 5.2.2 Slow-Drift Frequency

The second-order motion has a large amplitude and varies slowly in time, especially compared to the wave frequency motion. The time varying force component is oscillating in a horizontal manner, such as described in the preceding paragraph : $F_{top} = A\cos(\omega t + \Phi)$, where A is chosen to be *300 N* for all runs and where no phase difference $\Phi$ exists.

#### Convergence

The wave characteristics, used in the simulations, for the slow-drift component are defined in table (5.5). By comparison with the wave periods of table (5.4), the slow-drift period, considerably larger than the wave frequencies, corresponds to a slowly varying time dependency $\omega t$ compared to the wave frequencies.

Figure (5-11) and (5-12) show the slow-drift motion, at time $t = 0$ for a steel and synthetic cable. The number of elements, denoted by N on the plots, ranges from ten to fourty to show convergence.

| | | |
|---|---|---|
| Wave period **T** | = | 160 *s* |
| Wave frequency $\omega$ | = | 0.04 *rad/s* |

Table 5.5: Slow-drift properties

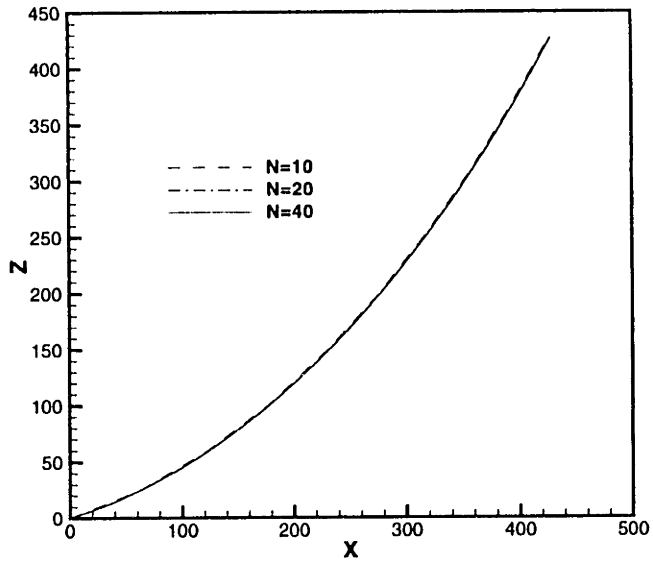


Figure 5-11: Convergence of the slow-drift displacement for a steel cable

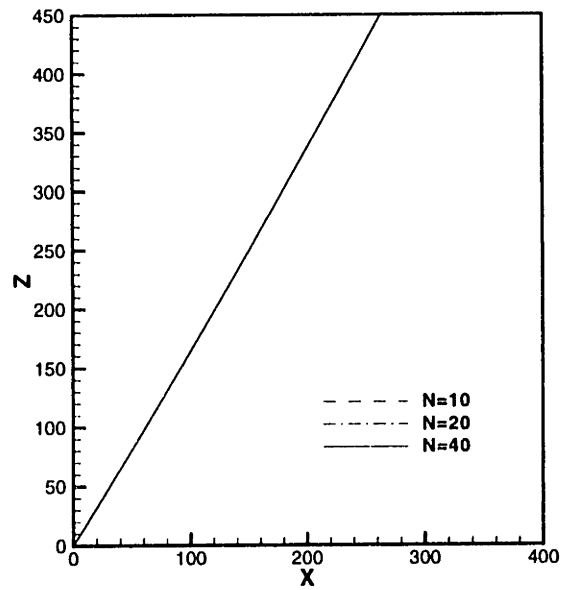


Figure 5-12: Convergence of the slow-drift displacement for a synthetic cable

The asymptotic value of the slow-drift case is reached quite rapidly. No changes are noticable for the cable displacement, for ten, twenty and fourty elements, therefore, convergence is verified with increasing number of elements for both materials. The same observation made for the wave frequency motion concerning the linear behavior of a synthetic cable versus the catenary shape form of a steel cable can also be made for the slow-drift motion.

### Cable Motion

The cable shape, defined by $\vec{r}(s,t) = \sum_{k=-n}^{n} \vec{C}_k(s)\ e^{ik\omega t}$, can be displayed at a given time t, by adding the coefficients $\vec{C}_k(s)$ for this chosen time t. The cable motion is then viewed by superposition of these snapshots over a period, or half a period, due to the symmetry of the motion. For large enough number of elements, i.e. for a fully converged case, snapshots of the cable motion at various times have been simulated over half a period. The resulting time dependent shape of the cable is showed in figures (5-13) and (5-14). Recall that the force is oscillated harmonically in the horizontal direction.

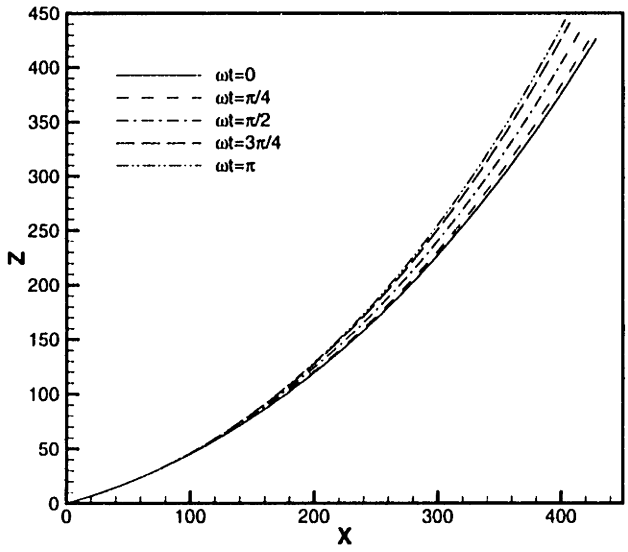


Figure 5-13: Slow-drift motion for a steel cable

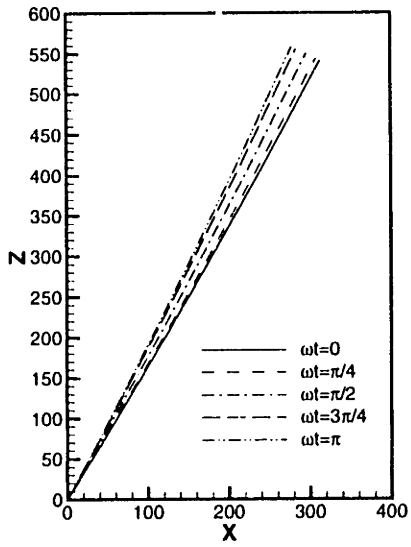


Figure 5-14: Slow-drift motion for a synthetic cable

Along the cable, from the bottom point to the top of the line, the slow-drift displacement decreases continuously over half a period, starting from its maximum at $\omega t = 0$ to its minimum for $\omega t = \pi$. The maximum amplitude of the slow-drift motion is observed over a half period, from the symmetry of the motion.

# CHAPTER 6

# CONCLUSION

The objective of this thesis was to investigate an approximate method based on multiple scale theory in order to model as efficiently as possible the dynamics of mooring lines. The first step was to decompose the motion of the cable into a mean static component, a wave frequency component, and a slow-drift component, each component characterized by the amplitude of their motion and their time dependency. The second step was to decompose into a Fourier series each component according to their time and space dependencies and under the assumption that the response of a stable physical system to a harmonic excitation is periodic. As a result, equations for these Fourier coefficients $\vec{C}_k$ have been derived. In addition, boundary conditions have also been specified in order to close the problem. Once the analytical problem was determined, the discretization and the resolution of these equations were performed based on a multidimensional rootfinding method. Numerical results have been obtained for the Fourier coefficients, leading to the prediction of the static and dynamic components of a mooring line motion. These results are presented first for the static case and then for the dynamic motion in chapter five.

The static case was proven to converge to results close to the the analytical solutions for both steel and synthetic cables. Therefore, the model based on the multiple scale theory and the Fourier analysis of the equation of motion has been validated for the static component for both materials. For the dynamic case, both wave and

slow-drift frequencies have been investigated. For both frequencies, the cable displacements of the numerical results were shown to converge to an asymptotic limit with an increasing number of elements for both materials. Several hybrid modes of the two dynamic motions were observed which result in the fully dynamic nature of the model. Finally, the effects of applying both a vertical and horizontal harmonic exciting force were examined.

The approach developed in this thesis is characterized by several advantages. First, the equations of motion for a mooring line solved by the method account for the complete non-linear structural effects. Second, it treats the fully dynamic motion of the cable, as opposed to other quasi-static methods. These effects are important for the behavior of offshore platforms, especially since mooring lines provide the only restoring forces in the horizontal plane for the slow-drift motion. In addition, coupling between wave and slow-drift frequencies can be performed for a small enough basis frequency $\omega$ and a large enough number of Fourier coefficients, if the wave frequency and the slow-drift frequency are multiples of the basis frequency. It would also be possible to model a realistic sea state to a certain extent. Since the problem was formulated in the frequency domain, with sufficiently high computer power, a whole wave spectrum could be handled by the program.

Further investigations would be usefull in order to model the fluid motion, which would require the addition of an exciting force distributed over the entire length of the cable. In addition, the viscous drag could be included in future developments. This aspect is essential for the evaluation of the damping due to mooring systems, which contribute significantly to the overall damping of the floating structure particularly for the slow-drift motion. Moreover, developments in the formulation of the boundary conditions could be made in order to take into account the varying length of the mooring line lying on the ocean floor from the anchor to the first point where the cable doesn't touch the bottom anymore. In addition, at the fairlead, a kinematic boundary condition specifying position at the top instead of an imposed force could be imposed. As a result, it would be easier to couple the mooring line model with with existing codes predicting the motion of offshore platforms.

# APPENDIX A

# DERIVATION OF THE APPROXIMATED EQUATIONS OF MOTION

## A.1 Dynamic motion

The vector position according to the Fourier decomposition is expressed by :

$$\vec{r}(s,t) = \sum_{k=-n}^{n} \vec{C}_k(s)\ e^{ik\omega t} \tag{A.1}$$

### A.1.1 Inertia of the mooring line

The acceleration term of the mooring line is given by :

$$\begin{aligned} \widetilde{M}\ddot{\vec{r}} &= (\rho_s A_s + \rho_f A_f C_m \mathcal{N})\,\ddot{\vec{r}} \\ &= (\rho_s A_s + \rho_f A_f C_m)\,\ddot{\vec{r}} - \rho_f A_f C_m \left(\vec{r'} \cdot \ddot{\vec{r}}\right) \vec{r'}. \end{aligned} \tag{A.2}$$

The term $\left(\vec{r}' \cdot \ddot{\vec{r}}\right)$ may be evaluated by combining eq.(A.1) with the identity given by (A.3).

$$\sum_{i=-n}^{n} a_i\, x^i \cdot \sum_{j=-m}^{m} b_j\, x^j \;=\; \sum_{l=-(n+m)}^{+(n+m)} \sum_{k=-n}^{n} a_k\, b_{l-k}\, x^l \tag{A.3}$$

where,

$$b_j \;=\; 0 \quad for\ j > m\ and\ j < -m,\ \ where\ |n| \geq |m| \tag{A.4}$$

The resulting expression for $\left(\vec{r}' \cdot \ddot{\vec{r}}\right)$ is :

$$\begin{aligned} \vec{r}' \cdot \ddot{\vec{r}} \;&=\; -\left(\sum_{k=-n}^{n} \vec{C}_k\, k^2\, \omega^2\; e^{ik\omega t}\right) \cdot \left(\sum_{l=-m}^{m} \vec{C}'_l\; e^{il\omega t}\right) \\ &=\; \sum_{p=-(n+m)}^{n+m} D_p\, e^{ip\omega t} \end{aligned} \tag{A.5}$$

where,

$$\begin{cases} D_p \;=\; -\omega^2 \sum_{q=-n}^{n} q^2\, \vec{C}_q \cdot \vec{C}'_{p-q} \\ \\ \vec{C}'_{p-q} \;=\; \vec{0} \quad for\ p-q > m\ and\ p-q < -m \end{cases} \tag{A.6}$$

Multiplying expression eq.(A.5) by $\vec{r}'$ results in :

$$\begin{aligned} \left(\vec{r}' \cdot \ddot{\vec{r}}\right) \vec{r}' \;&=\; \left(\sum_{p=-(n+m)}^{(n+m)} D_p\, e^{ip\omega t}\right) \left(\sum_{r=-m}^{m} \vec{C}'_r\; e^{ir\omega t}\right) \\ &=\; \sum_{s=-(n+2m)}^{(n+2m)} \vec{A}_s\; e^{is\omega t} \end{aligned} \tag{A.7}$$

where,

$$\begin{cases} \vec{A}_s &= \sum_{t=-(n+m)}^{(n+m)} D_t \vec{C}'_{s-t} \\ &= -\omega^2 \sum_{t=-(n+m)}^{(n+m)} \left( \sum_{q=-n}^{n} q^2 \, \vec{C}_q \cdot \vec{C}'_{t-q} \right) \vec{C}'_{s-t} \\ \vec{C}'_{s-t} &= \vec{0} \quad for \; s-t > m \; and \; s-t < -m \end{cases} \tag{A.8}$$

Substituting the preceding result eq.(A.7), and eq.(A.8), in the acceleration term eq.(A.2), and renaming the indices leads to :

$$\begin{aligned} \widetilde{M}\ddot{\vec{r}} &= -\left(\rho_s A_s + \rho_f A_f C_m\right) \omega^2 \sum_{s=-n}^{n} s^2 \, \vec{C}_s e^{is\omega t} \\ &+\rho_f A_f C_m \, \omega^2 \sum_{s=-(n+2m)}^{(n+2m)} \left[ \sum_{t=-(n+m)}^{(n+m)} \left( \sum_{q=-n}^{n} q^2 \, \vec{C}_q \cdot \vec{C}'_{t-q} \right) \vec{C}'_{s-t} \right] e^{is\omega t} \end{aligned} \tag{A.9}$$

The preceding expression can be simplified since $\ddot{\vec{r}}$ and $\vec{r}'$ both have the same number of Fourier coefficients, therefore $m = n$, and the inertia term of the cable, for a dynamic motion of frequency $\omega$ is given by :

$$\begin{aligned} \widetilde{M}\ddot{\vec{r}} &= -\left(\rho_s A_s + \rho_f A_f C_m\right) \omega^2 \sum_{s=-n}^{n} s^2 \, \vec{C}_s e^{is\omega t} \\ &+\rho_f A_f C_m \, \omega^2 \sum_{s=-3n}^{3n} \left[ \sum_{t=-2n}^{2n} \left( \sum_{q=-n}^{n} q^2 \, \vec{C}_q \cdot \vec{C}'_{t-q} \right) \vec{C}'_{s-t} \right] e^{is\omega t} \end{aligned} \tag{A.10}$$

where the conditions of existence for the Fourier coefficients are,

$$\begin{cases} \vec{C}'_{t-q} = \vec{0} \quad for\ t-q > n\ and\ t-q < -n \\ \\ \vec{C}'_{s-t} = \vec{0} \quad for\ s-t > n\ and\ s-t < -n \end{cases} \tag{A.11}$$

### A.1.2 Restoring of the mooring line

The effective tension $\tilde{\lambda}$ by :

$$\tilde{\lambda} = \frac{EA_s}{2}(\vec{r'} \cdot \vec{r'} - 1) \tag{A.12}$$

Also recall that :

$$\vec{r}(s,t) = \sum_{k=-n}^{n} \vec{C}_k(s)\ e^{ik\omega t}, \quad n \to +\infty \tag{A.13}$$

In order to obtain the developed form of $\tilde{\lambda}$ eq.(2.28), the following intermediate step is required :

$$\begin{aligned} \vec{r'} \cdot \vec{r'} &= \left( \sum_{k=-n}^{n} \vec{C}'_k\ e^{ik\omega t} \right) \cdot \left( \sum_{l=-m}^{m} \vec{C}'_l\ e^{il\omega t} \right) \\ &= \sum_{p=-(n+m)}^{(n+m)} E_p\ e^{ip\omega t} \end{aligned} \tag{A.14}$$

where,

$$\begin{cases} E_p = \sum_{q=-n}^{n} \vec{C}'_q \cdot \vec{C}'_{p-q} \\ \\ \vec{C}'_{p-q} = \vec{0} \quad for\ p-q > m\ and\ p-q < -m \end{cases} \tag{A.15}$$

Therefore, $\tilde{\lambda}$, (A.12) becomes :

$$\begin{aligned}\tilde{\lambda} &= P_f A_f + \frac{EA_s}{2}\left(\sum_{p=-(n+m)}^{(n+m)} E_p\, e^{ip\omega t} - 1\right) - P_e A_s \\ &= \left(P_f A_f - \frac{EA_s}{2} - P_e A_s\right) + \frac{EA_s}{2}\sum_{p=-(n+m)}^{(n+m)}\left(\sum_{q=-n}^{n}\vec{C}'_q \cdot \vec{C}'_{p-q}\right) e^{ip\omega t}\end{aligned} \tag{A.16}$$

The restoring term of the cable is then expressed by :

$$\begin{aligned}\left(\tilde{\lambda}\vec{r}'\right)' &= \left[\left(\frac{EA_s}{2}\sum_{p=-(n+m)}^{(n+m)} E_p\, e^{ip\omega t} + \left(P_f A_f - \frac{EA_s}{2} - P_e A_s\right)\right)\left(\sum_{r=-m}^{m}\vec{C}'_r\, e^{ir\omega t}\right)\right]' \\ &= \left[\frac{EA_s}{2}\sum_{s=-(n+2m)}^{(n+2m)}\vec{B}_s\, e^{is\omega t} + \left(P_f A_f - \frac{EA_s}{2} - P_e A_s\right)\sum_{r=-m}^{m}\vec{C}'_r\, e^{ir\omega t}\right]'\end{aligned} \tag{A.17}$$

where the coefficient $\vec{B}_s$ is given by,

$$\begin{cases}\vec{B}_s = \displaystyle\sum_{t=-(n+m)}^{(n+m)} D_t\, \vec{C}'_{s-t} \\ \qquad = \displaystyle\sum_{t=-(n+m)}^{+(n+m)}\left(\sum_{q=-n}^{n}\vec{C}'_q \cdot \vec{C}'_{t-q}\right)\vec{C}'_{s-t}\end{cases} \tag{A.18}$$

and the conditions on the coefficients $\vec{C}'_{t-q}$ and $\vec{C}'_{s-t}$ are,

$$\begin{cases}\vec{C}'_{t-q} = \vec{0} \quad for\ t-q > m\ and\ t-q < -m \\ \vec{C}'_{s-t} = \vec{0} \quad for\ s-t > m\ and\ s-t < -m\end{cases} \tag{A.19}$$

Finally, (A.17) becomes :

$$\begin{aligned}
\left(\tilde{\lambda}\vec{r}'\right)' &= \left(\left(P_f A_f - \frac{EA_s}{2} - P_e A_s\right) \sum_{s=-n}^{n} \vec{C}'_s e^{is\omega t} \right. \\
&\left. + \frac{EA_s}{2} \sum_{s=-(n+2m)}^{(n+2m)} \left[ \sum_{t=-(n+m)}^{+(n+m)} \left( \sum_{q=-n}^{n} \vec{C}'_q \cdot \vec{C}'_{t-q} \right) \vec{C}'_{s-t} \right] e^{is\omega t} \right)' \\
&= \left(P_f A_f - \frac{EA_s}{2} - P_e A_s\right) \sum_{s=-n}^{n} \vec{C}''_s e^{is\omega t} \\
&+ \frac{EA_s}{2} \sum_{s=-(n+2m)}^{(n+2m)} \left[ \sum_{t=-(n+m)}^{+(n+m)} \left( \sum_{q=-n}^{n} \vec{C}'_q \cdot \vec{C}'_{t-q} \right) \vec{C}'_{s-t} \right]' e^{is\omega t}
\end{aligned} \tag{A.20}$$

Obviously, $\vec{r}'$ and $\vec{r}'$ have the same Fourier decomposition, therefore $m = n$ and the restoring term for a motion of frequency $\omega$ becomes :

$$\begin{aligned}
\left(\tilde{\lambda}\vec{r}'\right)' &= \left(P_f A_f - \frac{EA_s}{2} - P_e A_s\right) \sum_{s=-n}^{n} \vec{C}''_s e^{is\omega t} \\
&+ \frac{EA_s}{2} \sum_{s=-3n}^{3n} \left[ \sum_{t=-2n}^{+2n} \left( \sum_{q=-n}^{n} \vec{C}'_q \cdot \vec{C}'_{t-q} \right) \vec{C}'_{s-t} \right]' e^{is\omega t}
\end{aligned} \tag{A.21}$$

where

$$\begin{cases}
\vec{C}'_{t-q} = \vec{0} \quad for\ t-q > m\ and\ t-q < -m \\
\vec{C}'_{s-t} = \vec{0} \quad for\ s-t > m\ and\ s-t < -m
\end{cases} \tag{A.22}$$

### A.1.3 Response of the mooring line

Substituting the inertia term eq.(A.9) and the restoring term eq.(A.20) into the left hand side of the general equation of motion eq.(2.6), results in the following :

$$\begin{aligned}
\widetilde{M}\vec{\ddot{r}} - (\tilde{\lambda}\vec{r}')' &= -(\rho_s A_s + \rho_f A_f C_m)\,\omega^2 \sum_{s=-n}^{n} s^2\,\vec{C}_s e^{is\omega t} \\
&\quad + \rho_f A_f C_m\,\omega^2 \sum_{s=-(n+2m)}^{(n+2m)} \left[ \sum_{t=-(n+m)}^{(n+m)} \left( \sum_{q=-n}^{n} q^2\,\vec{C}_q \cdot \vec{C}'_{t-q} \right) \vec{C}'_{s-t} \right] e^{is\omega t} \\
&\quad - \left( P_f A_f - \frac{EA_s}{2} - P_e A_s \right) \sum_{s=-n}^{n} \vec{C}''_s e^{is\omega t} \\
&\quad - \frac{EA_s}{2} \sum_{s=-(n+2m)}^{(n+2m)} \left[ \sum_{t=-(n+m)}^{+(n+m)} \left( \sum_{q=-n}^{n} \vec{C}'_q \cdot \vec{C}'_{t-q} \right) \vec{C}'_{s-t} \right]' e^{is\omega t}
\end{aligned} \tag{A.23}$$

where,

$$\begin{cases}
\vec{C}'_{t-q} = \vec{0} \quad for\ t-q > n\ and\ t-q < -n \\
\vec{C}'_{s-t} = \vec{0} \quad for\ s-t > n\ and\ s-t < -n
\end{cases} \tag{A.24}$$

Letting $m = n$ yields the final equation of the dynamic motion for a given frequency.

### A.1.4 Forces

The drag force is given by :

$$F_D = \frac{\rho_f}{2} C_d D_f \vec{v}_n^{rel} \left| \vec{v}_n^{rel} \right| \tag{A.25}$$

For a stationary fluid, the relative velocity yields :

$$\begin{cases} \vec{v}_n^{rel} &= -\mathcal{N}\vec{r} \\ &= -\left(\vec{r} - (\vec{r}\cdot\vec{r'})\vec{r'}\right) \end{cases} \tag{A.26}$$

Given the Fourier decomposition $\vec{r}(s,t) = \sum_{k=-n}^{n} \vec{C}_k(s)\ e^{ik\omega t}$, the developed form of $(\vec{r}\cdot\vec{r'})$ is :

$$\begin{aligned} \vec{r'}\cdot\vec{r} &= \left(i\,\omega \sum_{k=-n}^{n} \vec{C}_k\, k\ e^{ik\omega t}\right)\cdot\left(\sum_{l=-m}^{m} \vec{C}'_l\ e^{il\omega t}\right) \\ &= \sum_{p=-(n+m)}^{n+m} D_p\, e^{ip\omega t} \end{aligned} \tag{A.27}$$

where,

$$\begin{cases} D_p &= i\,\omega \sum_{q=-n}^{n} q\,\vec{C}_q\cdot\vec{C}'_{p-q} \\ \vec{C}'_{p-q} &= \vec{0} \quad for\ p-q > m\ and\ p-q < -m \end{cases} \tag{A.28}$$

Multiplying the preceding expression eq.(A.27) by $\vec{r'}$ yields :

$$\begin{aligned} \left(\vec{r'}\cdot\vec{r}\right)\vec{r'} &= \left(\sum_{p=-(n+m)}^{(n+m)} D_p\, e^{ip\omega t}\right)\left(\sum_{r=-m}^{m} \vec{C}'_r\ e^{ir\omega t}\right) \\ &= \sum_{s=-(n+2m)}^{(n+2m)} \vec{A}_s\ e^{is\omega t} \end{aligned} \tag{A.29}$$

where,

$$\begin{cases} \vec{A}_s &= \sum_{t=-(n+m)}^{(n+m)} D_t \vec{C}'_{s-t} \\ &= i\omega \sum_{t=-(n+m)}^{(n+m)} \left( \sum_{q=-n}^{n} q\, \vec{C}_q \cdot \vec{C}'_{t-q} \right) \vec{C}'_{s-t} \\ \vec{C}'_{t-q} &= \vec{0} \quad for\ t-q > m\ and\ t-q < -m \\ \vec{C}'_{s-t} &= \vec{0} \quad for\ s-t > m\ and\ s-t < -m \end{cases} \tag{A.30}$$

Or, for n = m,

$$\left(\vec{r}' \cdot \vec{r}\right) \vec{r}' = \sum_{s=-3n}^{3n} \vec{A}_s\, e^{is\omega t} \tag{A.31}$$

where,

$$\begin{cases} \vec{A}_s &= i\omega \sum_{t=-2n}^{2n} \left( \sum_{q=-n}^{n} q\, \vec{C}_q \cdot \vec{C}'_{t-q} \right) \vec{C}'_{s-t} \\ \vec{C}'_{t-q} &= \vec{0} \quad for\ t-q > m\ and\ t-q < -m \\ \vec{C}'_{s-t} &= \vec{0} \quad for\ s-t > n\ and\ s-t < -n \end{cases} \tag{A.32}$$

Therefore, the relative velocity $\vec{v}_n^{rel}$ becomes :

$$\vec{v}_n^{rel} = -i\omega \left( \sum_{k=-n}^{n} \vec{C}_k\, k\, e^{ik\omega t} - \sum_{s=-3n}^{3n} \left[ \sum_{t=-2n}^{2n} \left( \sum_{q=-n}^{n} q\, \vec{C}_q \cdot \vec{C}'_{t-q} \right) \vec{C}'_{s-t} \right] e^{is\omega t} \right) \tag{A.33}$$

with

$$\begin{cases} \vec{C}'_{t-q} = \vec{0} \quad for\ t-q > n\ and\ t-q < -n \\ \\ \vec{C}'_{s-t} = \vec{0} \quad for\ s-t > n\ and\ s-t < -n \end{cases} \tag{A.34}$$

Finally, considering the expression of the relative velocity eq.(A.33), the drag force is obtained :

$$\begin{aligned} F_D &= \frac{\rho_f}{2} C_d D_f \vec{v}_n^{rel} \left| \vec{v}_n^{rel} \right| \\ &= -i\omega^2 \frac{\rho_f}{2} C_d D_f \left( \sum_{k=-n}^{n} \vec{C}_k\, k\ e^{ik\omega t} - \sum_{s=-3n}^{3n} \left[ \sum_{t=-2n}^{2n} \left( \sum_{q=-n}^{n} q\, \vec{C}_q \cdot \vec{C}'_{t-q} \right) \vec{C}'_{s-t} \right] e^{is\omega t} \right) \\ &\quad \cdot \left| \sum_{k=-n}^{n} \vec{C}_k\, k\ e^{ik\omega t} - \sum_{s=-3n}^{3n} \left[ \sum_{t=-2n}^{2n} \left( \sum_{q=-n}^{n} q\, \vec{C}_q \cdot \vec{C}'_{t-q} \right) \vec{C}'_{s-t} \right] e^{is\omega t} \right| \end{aligned} \tag{A.35}$$

with the constraints given by eq.(A.34).

# Bibliography


[1] N.S. Asaithambi. *Numerical Analysis*, chapter 2,3,5,11. Saunders Cambridge Publishing, 1995.

[2] O.J. Emmerhoff and P.D. Sclavounos. The simulation of slow-drift motions of offshore structures. *Applied Ocean Research*, 18(2 & 3), 1996.

[3] D.L. Garrett. Dynamic analysis of slender rods. In *Proceedings of the first OMAE Conference*, pages 127–132, Dallas, 1982.

[4] S. Kim, P.D. Sclavounos, and F.G. Nielsen. Slow-drift responses of moored platforms. In $8^{th}$ *BOSS Conference, Netherlands*, July 1997.

[5] R.P. Nordgren. On computation of the motion of elastic rods. *Journal of Applied Mechanics*, pages 777–780, September 1974.

[6] J.R. Paulling and W.C. Webster. A consistent, large-amplitude analysis of the coupled response of a tlp and tendon system. In *Proceedings of the fifth OMAE Conference*, pages 126–133, Tokyo, 1986.

[7] W.H. Press, B.P. Flannery, S.A. Teukolsky, and W.T. Vetterling. *Numerical Recipes*, chapter 2.9. Cambrige University Press, 1990.

[8] A.A. Tjavaras. *The Dynamics of Highly Extensible Cables.* PhD dissertation, Massachusetts Institute of Technology, Department of Ocean Engineering, May 1996.

[9] W.C. Webster. Mooring-induced damping. *Ocean Engineering*, 22(6):571–591, 1995.